# Quantum Monte Carlo studies of relativistic effects in light nuclei

J. L. Forest* and V. R. Pandharipande†
*Department of Physics, University of Illinois at Urbana-Champaign, 1110 West Green Street, Urbana, Illinois 61801*

A. Arriaga‡
*Centro de Fisica Nuclear da Universidade de Lisboa, Avenida Gama Pinto 2, 1699 Lisboa, Portugal*
*and Departamento de Fisica, Faculdade de Ciências da Universidade de Lisboa, 1700 Lisboa, Portugal*
(Received 18 May 1998; published 16 June 1999)

Relativistic Hamiltonians are defined as the sum of relativistic one-body kinetic energy, two- and three-body potentials, and their boost corrections. In this work we use the variational Monte Carlo method to study two kinds of relativistic effects in $^3$H and $^4$He, using relativistic Hamiltonians. The first is due to the nonlocalities in the relativistic kinetic energy and relativistic one-pion exchange potential (OPEP), and the second is from boost interaction. The OPEP contribution is reduced by $\sim$15% by the relativistic nonlocality, which may also have significant effects on pion exchange currents. However, almost all of this reduction is canceled by changes in the kinetic energy and other interaction terms, and the total effect of the nonlocalities on the binding energy is very small. The boost interactions, on the other hand, give repulsive contributions of $\sim$0.4 (1.9) MeV in $^3$H ($^4$He) and account for $\sim$37% of the phenomenological part of the three-nucleon interaction needed in the nonrelativistic Hamiltonians. The wave functions of nuclei are not significantly changed by these effects. [S0556-2813(99)03607-9]

PACS number(s): 21.45.+v, 21.60.Ka, 24.10.Jv

## I. INTRODUCTION

It is generally accepted that QCD is the fundamental theory of strong interactions, however, due to quark confinement, the genuine QCD degrees of freedom are not explicit at low energies. In low-energy nuclear physics, nucleons and mesons are believed to be the physical (effective) degrees of freedom. In the nonrelativistic many-body theory, nuclei are regarded as bound states of nucleons interacting via two- and three-body potentials. All the subnucleonic and meson degrees of freedom, as well as relativistic effects are, in some way, absorbed in these potentials. Typically the nonrelativistic Hamiltonian is expressed as

$$H_{\rm NR}=\sum_i \frac{p_i^2}{2m_i}+\sum_{i<j} v_{ij}+\sum_{i<j<k} V_{ijk}+\cdots, \qquad (1.1)$$

and models of two- and three-body potentials are constructed by fitting observed data. The ellipsis in Eq. (1.1) represents $N$-body interactions ($N\geqslant 4$) which are thought to be much smaller than two- or three-nucleon interactions, and therefore neglected.

The central problem is to solve the many-body Schrödinger equation

$$H_{\rm NR}|\Psi\rangle = E|\Psi\rangle. \qquad (1.2)$$

The eigenvalues $E$ can be compared with experimental energies, and the eigenstates $|\Psi\rangle$ can be used both to study the nuclear structure and probe it through electron-nucleus scattering experiments, and to calculate rates of nuclear reactions which may have important applications in several domains of physics.

Schrödinger equation (1.2) is difficult to solve due to the large spin and isospin dependence of $v_{ij}$ and $V_{ijk}$. Several techniques have been developed, among which are Faddeev-Yakubovsky [1], harmonic-hyperspherical basis [2], and quantum Monte Carlo (QMC) [3,4] methods. The first two methods are limited to solving three- and four-nucleon systems, whereas with the third method it is now possible to calculate the ground state energy and wave function for $A=2$–$8$ nuclei with great accuracy.

Some of the results obtained by Pudliner *et al.* [5] are listed in Table I. The Argonne $v_{18}$ two-body potential [6], fitted to $NN$ scattering data and the deuteron binding energy, and Urbana IX three-body potential [5] constrained to give the correct binding energy of $^3$H and density of nuclear matter, are used in these calculations. It works rather well for $^4$He, however, as can be seen from Table I, the $A=6$, 7, and 8 nuclei appear to be systematically underbound. It is interesting to note that a large fraction of the total $v_{ij}$ comes from the one-pion exchange potential (OPEP) and the dominant part of $V_{ijk}$ comes from two-pion exchange. Also notice that the three-body interaction is much smaller than the two-body interaction, yet it is crucial to obtain the observed energies, because of the large cancellation between the kinetic energy and the two-body potential energy.

Although the nonrelativistic QMC techniques have advanced to such a level that the binding energies of light nuclei predicted by a realistic Hamiltonian can be calculated with $<1\%$ error [3,5], the effective description of nuclear dynamics by means of nonrelativistic Hamiltonians may

*Present address: Jefferson Lab Theory Group, 12000 Jefferson Ave., Newport News, VA 23606. Electronic address: jforest@jlab.org
†Electronic address: vijay@rsml.physics.uiuc.edu
‡Electronic address: arriaga@alf1.cii.fc.ul.pt

 

TABLE I. Nonrelativistic Green's function Monte Carlo (GFMC) results (in MeV) for light nuclei with the Argonne $v_{18}$ and Urbana IX potentials. The first line gives the experimental energy while the next four list the calculated total, kinetic, two-, and three-body interaction energies. The last two lines give the contribution of the pion exchange parts of two- and three-body interactions.

| | $^2$H | $^3$H | $^4$He | $^6$Li | $^7$Li | $^8$Be |
|---|---|---|---|---|---|---|
| $E_{\rm exp}$ | −2.2246 | −8.48 | −28.30 | −31.99 | −39.24 | −56.50 |
| $\langle E\rangle$ | −2.2248(5) | −8.47(1) | −28.30(2) | −31.25(11) | −37.44(28) | −54.66(64) |
| $\langle T\rangle$ | 19.81 | 50.8(5) | 111.9(6) | 150.8(10) | 186.4(28) | 246.3(56) |
| $\langle v_{ij}\rangle$ | −22.04 | −58.4(5) | −135.4(6) | −179.2(10) | −220.8(30) | −295.8(62) |
| $\langle V_{ijk}\rangle$ | 0.0 | −1.20(2) | −6.4(1) | −7.2(1) | −8.9(2) | −14.8(5) |
| $\langle v_\pi\rangle$ | −21.28 | −43.8(2) | −99.4(2) | −128.9(5) | −152.5(7) | −224.1(9) |
| $\langle V^{2\pi}\rangle$ | 0.0 | −2.17(1) | −11.7(1) | −13.5(1) | −17.1(4) | −28.1(8) |

have intrinsic deficiencies. In particular, when the nonrelativistic potentials are fit to the experimental data, relativistic effects are automatically buried in these potentials. How well can these effects be represented by means of local nonrelativistic potentials is an important question to be answered. In other words, we may investigate whether an explicit and more correct treatment of relativistic effects can resolve the systematic underbinding of the nonrelativistic results for $A=6,7,8$ nuclei. However, it is possible that this underbinding is not related to relativistic effects. In fact, significantly improved results of binding energies of $A\leqslant 8$ nuclei have been obtained with more realistic models of $V_{ijk}$ [7].

Furthermore, with the recently completed multi-GeV electron accelerator facilities such as TJNAF, experiments will be performed at energy and momentum transfer regimes where relativistic effects are substantial in kinetic energies and possibly in other aspects. Clearly, investigation of these effects in nuclear ground states is also necessary. Above all, no matter how small the relativistic effects might be, understanding them is a fundamental quest, just like understanding the fine and hyperfine structures in the hydrogen atom.

We have not yet arrived at a satisfactory relativistic theory of nuclei. That is a formidable task due to the internal quark structure of nucleons. Several approaches have been developed to study various relativistic effects that may occur in few-body nuclei. The calculations aim to provide an estimate of the magnitude of the effect studied, and learn from the available experimental data. The approaches can be classified in two main categories: effective field theories and relativistic Hamiltonian dynamics. Within the first one, the Bethe-Salpeter equations for the two- and three-body systems have been solved using a separable kernel [8]. Also covariant three-dimensional reductions of the relativistic integral equations have been applied, along with one-boson exchange models for the kernels, to the three-nucleon system. Here we refer to minimal relativity in the Blankenbecler-Sugar equations [9] and, more recently, to the spectator (Gross) equations [10]. In the relativistic Hamiltonian dynamics approach, relativistic covariance is achieved through the Poincaré group theory. One application of this method is the light front dynamics, which has been applied to the two-body system [11], and the other is the instant form.

The present interest in the relativistic Hamiltonian ($H_R$) dynamics in the instant form stems from the fact that the ground states of this Hamiltonian can be studied with the quantum Monte Carlo methods that have already been developed in the nonrelativistic approach. Earlier studies [12,13] and the present study are limited to the $A=2$, 3, and 4 nuclei, but attempts to study larger nuclei are in progress. Combinations of meson exchange and phenomenological terms can be used in the interactions in $H_R$, which allows a very good fit to the two-body scattering data with $\chi^2\sim 1$. It is improbable that the entire short and intermediate range two-nucleon interaction can be represented as due to the exchange of a few types of mesons. Therefore more general ways of studying relativistic effects in nuclei are desirable.

In this paper we report new results for the binding energies of the $A=3,4$ systems, using the relativistic Hamiltonian dynamics in the instant form, where for the first time the nonlocalities induced by the relativistic effects in the one-pion-exchange potential are taken into account. In Sec. II we describe the relativistic Hamiltonian used in this work, discuss the physical motivation behind its choice and the relativistic effects it contains in addition to those in the interactions of $H_{\rm NR}$. In Sec. III we apply variational Monte Carlo (VMC) techniques and present results. Finally we summarize in Sec. IV. Some of the detailed derivations involved in this work are given in the Appendix.

## II. THE RELATIVISTIC HAMILTONIAN

In relativistic Hamiltonian dynamics in instant form the momentum (**P**) and angular momentum (**J**) generators are chosen in the conventional way and therefore are independent of interaction, while the Hamiltonian ($H$) and boost (**K**) generators have interaction terms. Based on the pioneering work of Bakamjian and Thomas [14] and Foldy [15], the relativistic Hamiltonian can be expressed as

$$H_R=\sum_i\ (\sqrt{m_i^2+p_i^2}-m_i)+\sum_{i<j}\ [\tilde{v}_{ij}+\delta v_{ij}(\mathbf{P}_{ij})]$$
$$+\sum_{i<j<k}\ [\tilde{V}_{ijk}+\delta V_{ijk}(\mathbf{P}_{ijk})]+\cdots, \qquad (2.1)$$

where $\tilde{v}_{ij}$ are two-body potentials in the ''rest frame'' of particles $i$ and $j$ (i.e., the frame in which $\mathbf{P}_{ij}=\mathbf{p}_i+\mathbf{p}_j=0$).

Similarly $\tilde{V}_{ijk}$ is the three-body potential in the frame in which $\mathbf{P}_{ijk}=\mathbf{p}_i+\mathbf{p}_j+\mathbf{p}_k=0$. The $\delta v_{ij}(\mathbf{P}_{ij})$ and $\delta V_{ijk}(\mathbf{P}_{ijk})$ are called ''boost interactions'' and depend upon the total momentum of the interacting particles. Obviously, $\delta v_{ij}(\mathbf{P}_{ij}=0)$ and $\delta V_{ijk}(\mathbf{P}_{ijk}=0)$ vanish. The $\delta V_{ijk}(\mathbf{P}_{ijk})$ is neglected in the present work. It is believed to be much smaller than the terms considered.

We will now discuss the choice of the terms and interactions in the above relativistic Hamiltonian. This Hamiltonian is not yet derived from QCD, though we hope that in the future it may be possible to obtain it from QCD. We have also made no attempts to derive it from a Lagrangian containing nucleon and meson fields. Even though such a Lagrangian offers a useful language to discuss nuclear forces, it cannot possibly describe all aspects of nuclear forces since nucleons are bound states of quarks. For example, the exchange of electrons is known to be responsible for the binding of two hydrogen atoms to form the hydrogen molecule, as described by Heitler and London. It is not possible to represent this attraction as due to exchange of photons or Bosons such as the various positronium states, by the interacting atoms. There can be similar quark exchange interactions between nucleons that can not be described by meson exchange.

Due to the exceptionally small mass of pions, the long range interaction between nucleons is mediated only by pion exchange. This interaction can presumably be described by an effective field theory containing nucleon and pion fields. The OPEP in the $v_{ij}$ of $H_{\rm NR}$ is derived from the nonrelativistic $\boldsymbol{\sigma}\cdot\boldsymbol{\nabla}$ coupling of the pion field to nucleons, while that in the $\tilde{v}_{ij}$ of $H_R$ is obtained from relativistic pion-nucleon field theory as described below.

Parts of the intermediate range attraction are believed to be due to two-pion exchange processes including excitation of the nucleons to Delta- and higher-resonances. This process is analogous to the two-photon exchange, dipole-dipole, Van der Waals attraction between atoms. In the nucleon-meson field theory it is often represented by the exchange of a fictitious $\sigma$-meson. In effective field theories the short-range part is attributed to the exchange of vector mesons with mass of $\sim 780$ MeV. The quarks are confined to nucleons with flux tubes having a tension of $\sim 900$ MeV/fm. Therefore a valance quark can wander 1 fm away from the nucleon as easily as a vector meson, and the short-range interaction can have quark-exchange parts outside of the scope of nucleon-meson field theory. For these reasons all parts of the $v_{ij}$ and $\tilde{v}_{ij}$ in $H_{\rm NR}$ and $H_R$, other than OPEP are phenomenological. They obtain their quality only via accurate fits to the $NN$-scattering data. It is therefore absolutely essential that any $H_R$ used to test the accuracy of the predictions of $H_{\rm NR}$ must be accurately phase equivalent to the $H_{\rm NR}$. We assure this as described below.

The boost interaction $\delta v(\mathbf{P}_{ij})$ in the $H_R$ is totally neglected in the $H_{\rm NR}$. It is determined from the ''rest frame'' potential $\tilde{v}_{ij}$ through relativistic covariance [16,17]. The $\delta v(\mathbf{P}_{ij})$ is expanded in powers of $P_{ij}^2/4m^2$ and only the leading corrections are considered in this work for reasons discussed in Ref. [12] and in Sec. III D. This leading term is given by

$$\delta v(\mathbf{P})=-\frac{P^2}{8m^2}\tilde{v}+\frac{i}{8m^2}[\mathbf{P}\cdot\mathbf{r}\mathbf{P}\cdot\mathbf{p},\tilde{v}] + \frac{i}{8m^2}[(\boldsymbol{\sigma}_1-\boldsymbol{\sigma}_2)\times\mathbf{P}\cdot\mathbf{p},\tilde{v}], \tag{2.2}$$

where the subscripts $ij$ of $\tilde{v}$, $\mathbf{P}$, $\mathbf{p}$, and $\mathbf{r}$ have been suppressed for brevity. Here $\mathbf{p}=(\mathbf{p}_i-\mathbf{p}_j)/2$ is the relative momentum operator, and $\boldsymbol{\sigma}=2\mathbf{s}$ are the Pauli matrices for spin 1/2 particles.

Various aspects of $\delta v(\mathbf{P})$ are discussed in Ref. [18]. The first two terms of Eq. (2.2) are denoted as $\delta v_{\rm RE}$ and $\delta v_{\rm LC}$; they have simple classical origins in the relativistic energy-momentum relation and Lorentz contraction. The last term contains contributions from Thomas precession and quantum effects. They are denoted as $\delta v_{\rm TP}$ and $\delta v_{\rm QM}$ and are much smaller than the first two terms. For example, the contributions of $\delta v_{\rm RE}$, $\delta v_{\rm LC}$, $\delta v_{\rm TP}$, and $\delta v_{\rm QM}$ to the energy of triton are found [12] to be 0.23(2), 0.10(1), 0.016(2), and $-0.004(2)$ MeV, respectively. Since the main contribution comes from the first two terms, for simplicity, we neglected the last two terms in the three-, four-body calculations in this work.

All realistic models of nuclear forces contain terms with $p_{ij}^2$ dependence as dictated by the scattering data. If the nonrelativistic Hamiltonian is defined as that which contains all terms of order $p_i^2$, then it must contain these interactions as well as the boost interaction. It is useful to consider a familiar example. The Coulomb-Breit electromagnetic interaction [19] between two particles of mass $m$ and charge $Q$, ignoring spin dependent terms for brevity, is given by

$$v(\mathbf{p}_i,\mathbf{p}_j)=\frac{Q^2}{r_{ij}}\left(1-\frac{\mathbf{p}_i\cdot\mathbf{p}_j}{2m^2}-\frac{\mathbf{p}_i\cdot\mathbf{r}_{ij}\mathbf{p}_j\cdot\mathbf{r}_{ij}}{2m^2r_{ij}^2}\right), \tag{2.3}$$

up to terms quadratic in the velocities of the interacting particles. In our notation it is expressed as

$$v(\mathbf{p}_i,\mathbf{p}_j)=\tilde{v}_{ij}+\delta v(\mathbf{P}_{ij}), \tag{2.4}$$

with

$$\tilde{v}_{ij}=\frac{Q^2}{r_{ij}}\left[1+\frac{p_{ij}^2}{2m^2}+\frac{(\mathbf{p}_{ij}\cdot\mathbf{r}_{ij})^2}{2m^2r_{ij}^2}\right], \tag{2.5}$$

$$\delta v(\mathbf{P}_{ij})=-\frac{Q^2}{r_{ij}}\left[\frac{P_{ij}^2}{8m^2}+\frac{(\mathbf{P}_{ij}\cdot\mathbf{r}_{ij})^2}{8m^2r_{ij}^2}\right]. \tag{2.6}$$

It is obviously inconsistent to include only the terms of order $p_{ij}^2$, as most realistic nonrelativistic nuclear Hamiltonians do, and neglect the boost interaction of order $P_{ij}^2$. Unfortunately, even though contributions of the boost interaction to the binding energy of nuclear matter and $^3$H were estimated by

Coester and co-workers years ago [20,21], they have been neglected in most subsequent studies.

The $H_R$ requires, apart from obvious relativistic kinetic energy, a consistency between the rest frame $\tilde{v}$ and the boost interaction given by Eq. (2.2). If parts of $\tilde{v}$ can be derived from field theory, we can add them to other phenomenological parts to obtain the total $\tilde{v}$. Here we take the OPEP part of $\tilde{v}$ from relativistic field theory. This, together with the boost interaction it generates, include all the nonstatic terms in the OPEP predicted by relativistic pion-nucleon field theory as shown in Ref. [18].

It is interesting to compare the descriptions of known systems or models given by $H_{\rm NR}$ and $H_R$ to identify the relativistic effects contained in $H_R$ beyond those in the interactions of $H_{\rm NR}$. The simplest system is the hydrogen atom. The $H_{\rm NR}$ with only the Coulomb potential gives results correct up to order $\alpha^2$. Some of the terms, such as the magnetic interactions, Darwin correction, etc., which give corrections of order $\alpha^4$, can be included in the $H_{\rm NR}$ by adding the appropriate interactions to $v_{ij}$. However, the $H_{\rm NR}$ does not give the correct energy up to order $\alpha^4$ because the $p^4/8m^3$ correction to the nonrelativistic kinetic energy omitted in the $H_{\rm NR}$ gives a contributions of order $\alpha^4$. The $H_R$, with a proper choice of $\tilde{v}$, gives results correct to order $\alpha^4$. We have not examined the reproducibility of the $\alpha^6$ correction by an $H_R$.

Next, we can consider the hypothetical system known as the Walecka model of nuclear matter. The problem of extended uniform matter consisting of Dirac particles interacting with long-range scalar and vector fields has been solved by Serot and Walecka [22] in the mean field limit. The approximate solutions to this problem obtained with $H_R$ and $H_{\rm NR}$ have been discussed in Ref. [18]. With appropriate choice of $v_{ij}$ the $H_{\rm NR}$ can reproduce terms in the expansion of the energy per particle, of order up to $k_F^3$. The term of order $k_F^4$ comes from the relativistic correction to the kinetic energy while that of order $k_F^5$ contains boost correction, both of which are absent in the $H_{\rm NR}$. The $H_R$ will reproduce all the terms up to order $k_F^{10}$. It is essential to include the boost correction of order $P^2$, as given by Eq. (2.2), to obtain the correct contribution of order $k_F^5$. The three-body force contribution is needed for the term of order $k_F^8$, while boost corrections of higher order than considered here are essential to reproduce terms of order $k_F^7$, $k_F^9$, and $k_F^{10}$. Four-body forces, neglected in Eq. (2.1), give contributions of order $k_F^{11}$. Three- and more-particle interactions originate only from the scalar field.

In both the examples considered above $H_R$ gives a substantial improvement over $H_{\rm NR}$. In these examples the difference between the results obtained with $H_R$ and $H_{\rm NR}$ gives the leading relativistic effect neglected in $H_{\rm NR}$. However, these systems are much simpler than nuclei. In Sec. IV we will argue that the $H_R$ may contain the leading relativistic correction to nuclear energies.

In the remainder part of this section we discuss the choice of the OPEP and $\tilde{v}$ in the $H_R$. The main focus of this work is on the treatment of OPEP in $H_R$; the calculation of boost interaction and relativistic kinetic energy has been described in detail in Refs. [18,12,13]. In most existing nonrelativistic potential models, the OPEP has been calculated using the nonrelativistic $\boldsymbol{\sigma}\cdot\boldsymbol{\nabla}$ coupling. Without $\pi NN$ form factors, it is given in momentum space by

$$\tilde{v}_{\pi,\rm NR}(\mathbf{q}) = -\frac{f_{\pi NN}^2}{\mu^2}\frac{\boldsymbol{\sigma}_i\cdot\mathbf{q}\boldsymbol{\sigma}_j\cdot\mathbf{q}\boldsymbol{\tau}_i\cdot\boldsymbol{\tau}_j}{\mu^2+q^2}, \tag{2.7}$$

where $f_{\pi NN}$ is the pion-nucleon coupling constant, $\mu$ is the pion mass, and $\mathbf{q}$ is the momentum transfer

$$\mathbf{q}=\mathbf{p}-\mathbf{p}'. \tag{2.8}$$

Here $\mathbf{p}$ and $\mathbf{p}'$ are the initial and final momenta of nucleon $i$ in the center of mass frame, and the $\tilde{v}_{\pi,\rm NR}$ is local, i.e., it depends only on $\mathbf{q}$.

In contrast, the OPEP in effective pion-nucleon relativistic field theories has the form

$$\tilde{v}_{\pi,\rm rel}(\mathbf{p}',\mathbf{p}) = \frac{m}{\sqrt{m^2+p'^2}}\,\tilde{v}_{\pi,\rm NR}(\mathbf{q})\frac{m}{\sqrt{m^2+p^2}}. \tag{2.9}$$

This potential is dependent not only on $\mathbf{q}$ but also on $\mathbf{p}$ and $\mathbf{p}'$, which results in a nonlocal potential in the configuration space. The interaction (2.9) is regarded as energy independent and used in many-body Schrödinger equations. By expanding the square roots it can be easily verified that the leading correction $(\tilde{v}_{\pi,\rm rel}-\tilde{v}_{\pi,\rm NR})$ is of order $p^2/m^2$, i.e., of order $v^2/c^2$ where $v$ denotes the velocity of the nucleons in the center of mass frame.

In the $H_R$ the $\tilde{v}_{\pi,\rm rel}(\mathbf{p}',\mathbf{p})$ is used for all $p^2$ and $p'^2$, whereas in the physically allowed one-pion exchange two nucleon scattering $p'^2$ must equal $p^2$ to conserve energy. When $p^2=p'^2$ (on shell), Eq. (2.9) is obtained with either pseudoscalar or pseudovector $\pi$-$N$ couplings and is considered to be model independent, apart from form factors, etc. The off-shell ($p^2\neq p'^2$) behavior of the OPEP is model dependent. It can be changed by using combinations of pseudoscalar and pseudovector couplings. In Friar's notation [23,24] the possible off-shell behaviors are characterized with parameters $\tilde{\mu}$ and $\nu$, and up to order $p^2/m^2$ they are related by unitary transformations. Our $\tilde{v}_{\pi,\rm rel}$ has an off-shell behavior with $\nu=1/2$ and $\tilde{\mu}=0$. In contrast the OPEP in the CD-Bonn model has the form

$$\tilde{v}_{\pi,\rm CDB}(\mathbf{p}',\mathbf{p}) = -\frac{f_{\pi NN}^2}{\mu^2}\frac{\boldsymbol{\tau}_i\cdot\boldsymbol{\tau}_j}{\mu^2+q^2}\frac{m}{E}\frac{m}{E'}\left[\boldsymbol{\sigma}_i\cdot\mathbf{q}\boldsymbol{\sigma}_j\cdot\mathbf{q} + (E'-E)\left(\frac{\boldsymbol{\sigma}_i\cdot\mathbf{p}\boldsymbol{\sigma}_j\cdot\mathbf{p}}{E+m}-\frac{\boldsymbol{\sigma}_i\cdot\mathbf{p}'\boldsymbol{\sigma}_j\cdot\mathbf{p}'}{E'+m}\right)\right], \tag{2.10}$$

obtained from pseudoscalar coupling [25,26]. Here $E=\sqrt{m^2+p^2}$, $E'=\sqrt{m^2+p'^2}$. The term proportional to $(E'-E)$ does not contribute to the on-shell OPEP, and is absent from the $\tilde{v}_{\pi,\rm rel}$ given by Eq. (2.9). In Friar's notation $\tilde{v}_{\pi,\rm CDB}$

has $\nu=1/2$ and $\tilde{\mu}=-1$. In principle, since the various OPEP are related to each other by a unitary transformation, originating from the Dyson transformation [27], the final answers should not depend upon the choice of $\tilde{\mu}$ and $\nu$. However, the current operators as well as the $V_{ijk}$ will depend upon the choice made [27]. Our choice is made primarily for the sake of simplicity, and for avoiding the complications of undoing the unphysical effects of the strong coupling between pions and nucleon-antinucleon pairs in the pseudoscalar theory.

In Ref. [18] it is shown that the relation between the boost interaction $\delta v(\mathbf{P})$ and the static $\tilde{v}_{\rm NR}$ is independent of the origin of $\tilde{v}_{\rm NR}$ up to order $P^2/m^2$, and thus the knowledge of the static $\tilde{v}_{\rm NR}$ is sufficient to obtain $\delta v(\mathbf{P})$. In contrast the relation [Eq. (2.9)] between $\tilde{v}_{\pi,\rm rel}$ and $\tilde{v}_{\pi,\rm NR}$ is specific for the interaction due to exchange of pseudoscalar mesons by nucleons represented by Dirac spinors via either pseudoscalar or pseudovector coupling. By expanding the square roots in Eq. (2.9) we obtain

$$\tilde{v}_{\pi,\rm rel}(\mathbf{p}',\mathbf{p})=\tilde{v}_{\pi,\rm NR}(\mathbf{q})\left(1-\frac{p'^2}{2m^2}-\frac{p^2}{2m^2}+\cdots\right), \tag{2.11}$$

whereas the interactions generated by exchange of scalar ($S$) or vector ($V$) mesons have different relations [18]:

$$\tilde{v}_{S,\rm rel}(\mathbf{p}',\mathbf{p})=\tilde{v}_{S,\rm NR}(\mathbf{q})\left(1-\frac{(\mathbf{p}'+\mathbf{p})^2}{2m^2}+\cdots\right), \tag{2.12}$$

$$\tilde{v}_{V,\rm rel}(\mathbf{p}',\mathbf{p})=\tilde{v}_{V,\rm NR}(\mathbf{q})\left(1+\frac{(\mathbf{p}'+\mathbf{p})^2}{2m^2}+\cdots\right). \tag{2.13}$$

Realistic models of nuclear forces contain momentum dependent central forces. However, most configuration space models do not contain long range, momentum dependent tensor forces occurring in $\tilde{v}_{\pi,\rm rel}$. In exact calculations the tensor force can not be generally expanded in powers of $p^2/m^2$. In any truncated expansion the force diverges at large values of $p$, and can yield divergent attraction. This poses the main technical challenge addressed in the present work.

The two-nucleon potential is expressed as

$$\tilde{v}_{NN}=\tilde{v}_{\pi,\rm rel}+\tilde{v}_R, \tag{2.14}$$

where $\tilde{v}_R$ is the remaining part of the two-body potential which is phenomenological. We can also write the OPEP given in Eq. (2.9) as

$$\tilde{v}_{\pi,\rm rel}=\tilde{v}_{\pi,\rm NR}+(\tilde{v}_{\pi,\rm rel}-\tilde{v}_{\pi,\rm NR}). \tag{2.15}$$

The term in parentheses is the relativistic correction. The nonrelativistic potential models do not consider this correction explicitly: the data is fit using $\tilde{v}_{\pi,\rm NR}$ in Eq. (2.14), thus some of its effects go into the phenomenological part of the potential $\tilde{v}_R$. The $\tilde{v}_R$ in relativistic Hamiltonian differs from that in nonrelativistic Hamiltonian due to the difference in $\tilde{v}_{\pi,\rm rel}$ and $\tilde{v}_{\pi,\rm NR}$ as well as that in the kinetic energy operators.

We construct our $H_R$ to be phase equivalent to the isoscalar part of the nonrelativistic $H_{\rm NR}$ containing Argonne $v_{18}$. The relativistic effects can then be studied by comparing results obtained from our $H_R$ and the isoscalar $H_{\rm NR}$ without considering the small isospin symmetry breaking terms in the latter. The relativistic Hamiltonian for two-nucleon system in its center of mass frame is

$$H_R=2\sqrt{p^2+m^2}-2m+\frac{m}{\sqrt{m^2+p'^2}}\tilde{v}_{\pi,\rm NR}(\mathbf{q})\frac{m}{\sqrt{m^2+p^2}}+\tilde{v}_R, \tag{2.16}$$

where $\tilde{v}_R$ has the same form as the isoscalar part of Argonne $v_{18}$ [6]:

$$\tilde{v}_R=\sum_{p=1,14} v_p(r_{ij})O_{ij}^p, \tag{2.17}$$

$$\begin{aligned} O_{ij}^{p=1,14}=&1,\boldsymbol{\tau}_i\cdot\boldsymbol{\tau}_j,\boldsymbol{\sigma}_i\cdot\boldsymbol{\sigma}_j,(\boldsymbol{\sigma}_i\cdot\boldsymbol{\sigma}_j)(\boldsymbol{\tau}_i\cdot\boldsymbol{\tau}_j),\\ &\times S_{ij},S_{ij}(\boldsymbol{\tau}_i\cdot\boldsymbol{\tau}_j),\mathbf{L}\cdot\mathbf{S},\mathbf{L}\cdot\mathbf{S}(\boldsymbol{\tau}_i\cdot\boldsymbol{\tau}_j),\\ &L^2,L^2(\boldsymbol{\tau}_i\cdot\boldsymbol{\tau}_j),L^2(\boldsymbol{\sigma}_i\cdot\boldsymbol{\sigma}_j),L^2(\boldsymbol{\sigma}_i\cdot\boldsymbol{\sigma}_j)(\boldsymbol{\tau}_i\cdot\boldsymbol{\tau}_j),\\ &\times(\mathbf{L}\cdot\mathbf{S})^2,(\mathbf{L}\cdot\mathbf{S})^2(\boldsymbol{\tau}_i\cdot\boldsymbol{\tau}_j). \end{aligned} \tag{2.18}$$

The $\tilde{v}_{\pi,\rm NR}$ used in Argonne $v_{18}$ is given by

$$\tilde{v}_{\pi,\rm NR}(\mathbf{r})=\frac{1}{3}\mu\frac{f_{\pi NN}^2}{4\pi}[Y_\pi(r)\boldsymbol{\sigma}_i\cdot\boldsymbol{\sigma}_j+T_\pi(r)S_{ij}]\boldsymbol{\tau}_i\cdot\boldsymbol{\tau}_j, \tag{2.19}$$

where

$$Y_\pi(r)=\frac{e^{-\mu r}}{\mu r}(1-e^{-cr^2}), \tag{2.20}$$

$$T_\pi(r)=\left(1+\frac{3}{\mu r}+\frac{3}{(\mu r)^2}\right)(1-e^{-cr^2})^2, \tag{2.21}$$

$$S_{ij}=3\boldsymbol{\sigma}_i\cdot\hat{r}\boldsymbol{\sigma}_j\cdot\hat{r}-\boldsymbol{\sigma}_i\cdot\boldsymbol{\sigma}_j. \tag{2.22}$$

We note that this $\tilde{v}_{\pi,\rm NR}$ does not contain the part of $\boldsymbol{\sigma}_i\cdot\boldsymbol{\sigma}_j\boldsymbol{\tau}_i\cdot\boldsymbol{\tau}_j$ interaction which acquires a $\delta(r_{ij})$ function form in the limit of point particles. This $\delta$ function is probably spread out by the finite size of the nucleons, and contributes to the short range part of $v_{NN}$. However, it is difficult to extract it from the phenomenological models. Moreover the dominant contribution and the nonlocality effect seem to come from the tensor part of OPEP.

Recently, after completion of the present work, Kamada and Glöckle [28] found an elegant method to obtain a potential $v_{\rm rel}$ that gives exactly the same phase shifts with relativistic kinetic energy that a known $v_{\rm NR}$ gives with nonrelativ-

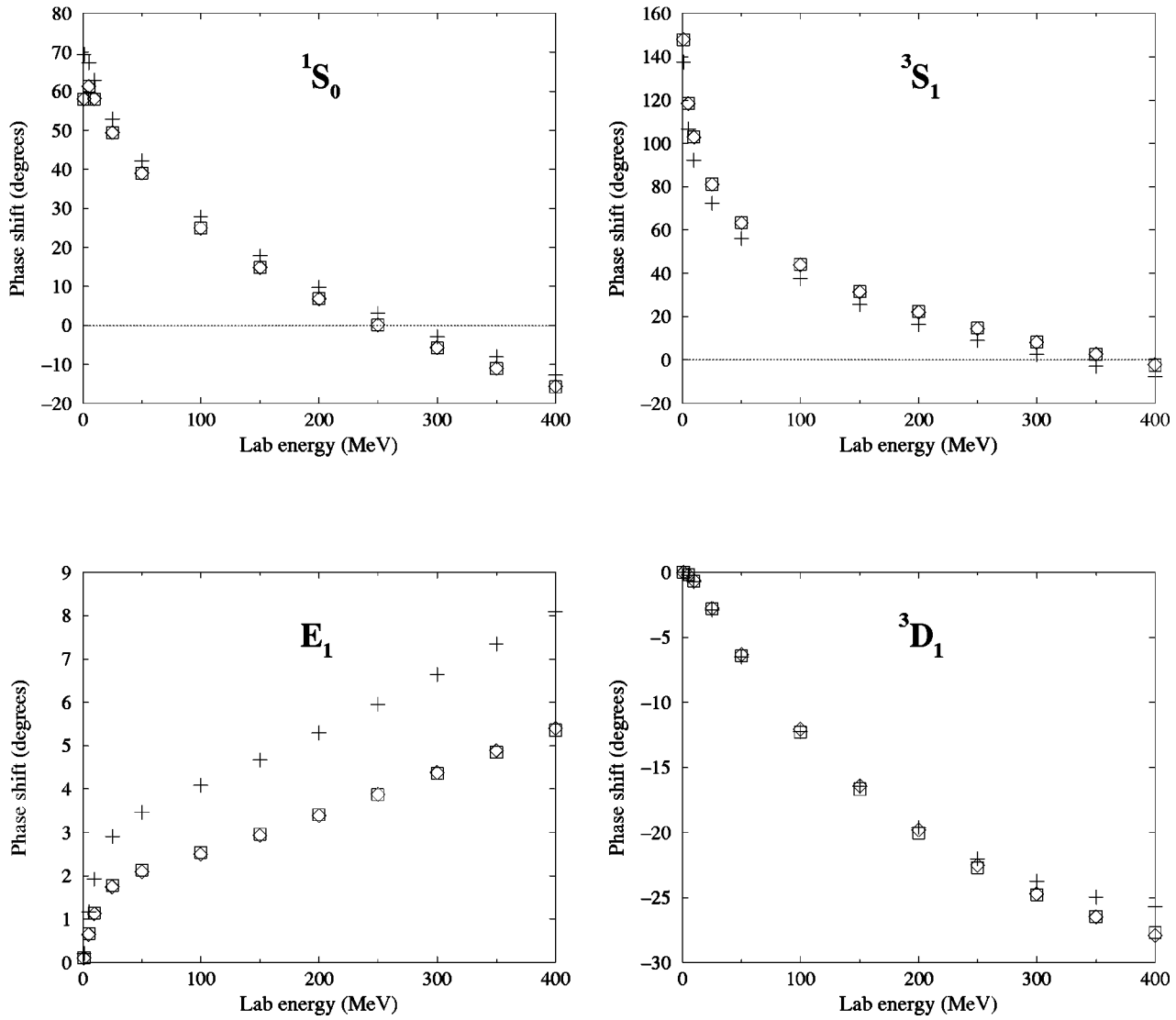


FIG. 1. Phase shifts as a function of lab energy. $\diamond$ : the reference phase shifts obtained with $H_{\rm NR}$ ; $+$ : those using $\tilde{v}_R$ from $H_{\rm NR}$ in $H_R$ ; $\square$ : those with the new relativistic Hamiltonian $H_R$ with readjusted $\tilde{v}_R$ .

istic kinetic energy. Our objective here is not just to find a $v_{\rm rel}$ that is phase equivalent to the Argonne $v_{18}$ ; we additionally require it to have the $\tilde{v}_{\pi,{\rm rel}}$ long range behavior. Both relativistic and nonrelativistic models of $\tilde{v}$ contain theoretical long range OPEP; the scattering data is used to determine only the phenomenological part $\tilde{v}_R$ in these interactions. Our two models are not as exactly phase equivalent as Kamada and Glöckle's $v_{\rm rel}$ and $v_{\rm NR}$ are, however the differences in their phase shifts are negligibly small compared to the uncertainties in the Nijmegen phase shifts [29].

The parameters of the function $v_p(r_{ij})$ of $\tilde{v}_R$ are obtained by fitting the phase shifts and deuteron binding energy. Traditionally phase shifts are calculated in configuration space, however, in the relativistic case, the Hamiltonian contains $\sqrt{m^2-\nabla^2}$ which is nonlocal in configuration space, therefore we calculate them in momentum space. The details of the momentum-space technique have been discussed in Ref. [30].

Some of the important phase shifts are plotted in Fig. 1. The diamond symbols represent the reference nonrelativistic phase shifts obtained with $H_{\rm NR}$, the plus symbols represent those calculated from $H_R$ before readjusting the parameters in $v_p(r)$, and the square symbols correspond to those after. The reference phase shifts are almost exactly reproduced by the relativistic Hamiltonian $H_R$ as indicated by the good overlap of the diamond and square symbols in Fig. 1. The deviations between the plus and diamond symbols reflect the total effect of replacing nonrelativistic kinetic energy and

TABLE II. Deuteron properties.

| | $H_{\rm NR}$ | $H_R$ |
|---|---|---|
| binding energy (MeV) [a] | −2.242 | −2.242 |
| quadrupole moment (fm$^2$) | 0.269 | 0.271 |
| % of $D$ state ($P_D$) | 5.776 | 5.732 |

[a]Without electromagnetic interactions.

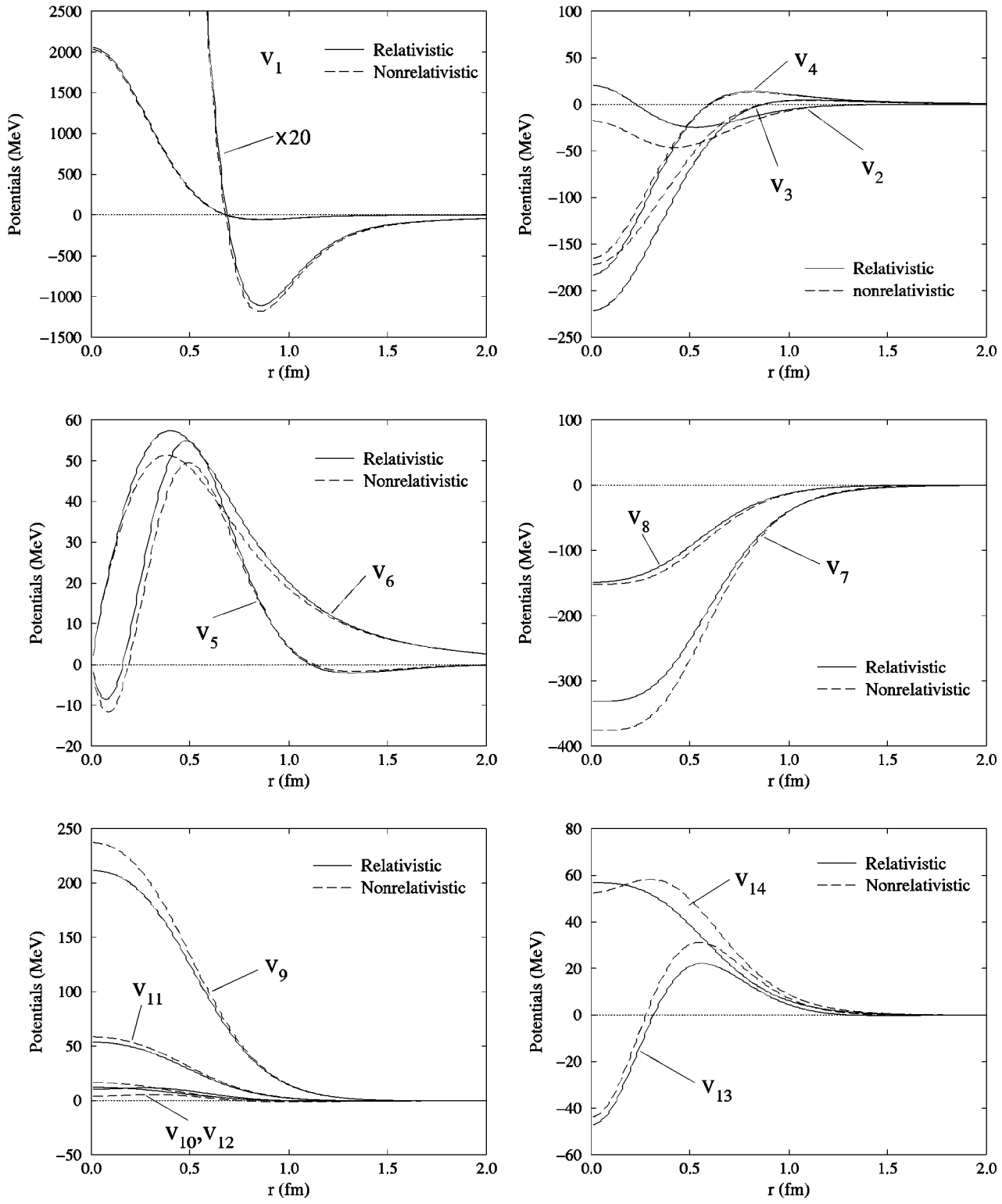


FIG. 2. Comparison of relativistic (solid lines) and nonrelativistic (dashed lines) potentials $v_1-v_{14}$ of the operator format [refer to Eq. (2.17)]. Note that $v_4$ and $v_6$ contain contributions from both $\tilde{v}_\pi$ and $\tilde{v}_R$, and only a local nonrelativistic OPEP is used.

$\tilde{v}_{\pi,\mathrm{NR}}$ by the relativistic kinetic energy and $\tilde{v}_{\pi,\mathrm{rel}}$ in $H_{\mathrm{NR}}$, and are not too large except for the mixing parameter $E_1$ of $^3S_1-{}^3D_1$. This indicates that relativistic nonlocal effects in two nucleon scattering at $E_{\mathrm{lab}}<400$ MeV are rather small. $E_1$ is primarily determined by the tensor force; the relatively large change in $E_1$ is due to the nonlocality of the tensor force in $\tilde{v}_{\pi,\mathrm{rel}}$.

The new two-body potential is essentially phase equivalent to isoscalar part of Argonne $v_{18}$ and predicts similar deuteron properties as listed in Table II. Note that the present

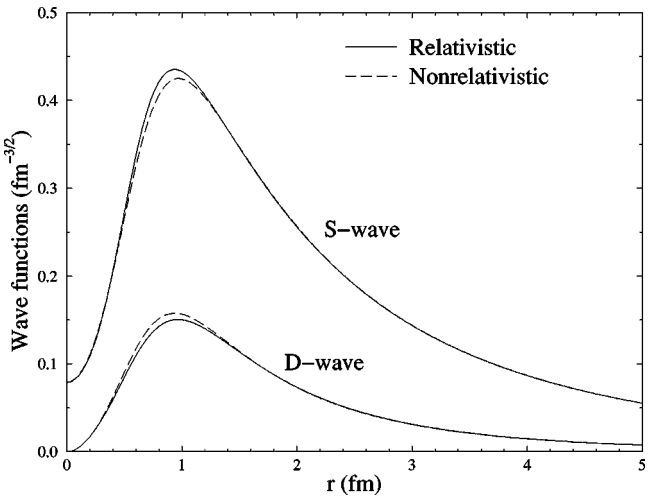


FIG. 3. Deuteron wave functions.

$H_{\rm NR}$ and $H_R$ do not contain electromagnetic interactions. The experimental value of deuteron binding energy ($-2.224$ MeV) can be obtained from the full Argonne $v_{18}$ with electromagnetic interactions. The 14 operator components of the relativistic and nonrelativistic potentials are compared in Fig. 2. Only the static part of the relativistic OPEP, obtained by setting $m/\sqrt{p^2+m^2}$ equal to unity is used in Fig. 2. Since it is the same as the nonrelativistic OPEP, the difference between the potentials shown in the figure is entirely due to that in the phenomenological part $\tilde{v}_R$. Equation (2.9) shows that the $\tilde{v}_{\pi,\rm rel}$ is smaller than the $\tilde{v}_{\pi,\rm NR}$ for $p$ or $p' \neq 0$.

The deuteron *S*- and *D*-wave functions are shown in Fig. 3. Here the relativistic *D* wave is slightly smaller than the nonrelativistic one, presumably because the relativistic tensor potential is smaller than the nonrelativistic tensor potential [Eq. (2.9)] for large $p$ and $p'$. The deuteron wave functions in momentum space are shown in Fig. 4. Note that the relativistic wave functions are not very different from the nonrelativistic ones. The ratio of the two momentum space *D*-wave functions can be easily understood as discussed below.

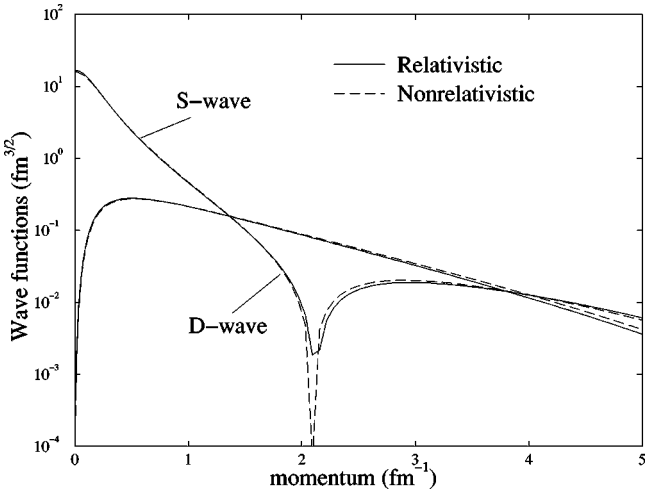


FIG. 4. Deuteron wave functions in momentum space.

The exact ground state wave function $\Psi$ can be expanded in a complete set of states $|i\rangle$:

$$|\Psi\rangle = \sum_i \phi_i |i\rangle. \tag{2.23}$$

For a Hamiltonian given by $T+v$, where $|i\rangle$ are eigenstates of $T$, the amplitudes $\phi_i$ are given by

$$\phi_i = -\frac{\langle i|v|\Psi\rangle}{\langle i|T-E_0|i\rangle}, \tag{2.24}$$

as can be verified from the Schrödinger equation $H|\Psi\rangle = E_0|\Psi\rangle$. Here $E_0$ is the ground state energy.

In the case of the deuteron we can choose $T$ as the kinetic energy operator and $|i\rangle$ as *S* and *D* waves with momentum $p$, denoted by $|p_l\rangle$, for $l=S,D$. The amplitudes $\phi_l(p)$ of these waves give the deuteron wave function in momentum space. We can estimate the difference between the nonrelativistic and relativistic deuteron *D*-state wave function at large momentum by assuming that it is primarily generated by the OPEP. In the nonrelativistic case this gives

$$\phi_{D,\rm NR}(p) = -\frac{m}{p^2}\langle p_D|\tilde{v}_{\pi,\rm NR}|\Psi\rangle, \tag{2.25}$$

where we have neglected the $E_0$ in the denominator of Eq. (2.24), since it is much smaller than the kinetic energy $p^2/m$ at large $p$. In the relativistic case

$$\phi_{D,\rm rel}(p) = -\frac{1}{2(\sqrt{m^2+p^2}-m)}\frac{m}{\sqrt{m^2+p^2}}\langle p_D|\tilde{v}_{\pi,\rm NR}|\Psi\rangle, \tag{2.26}$$

where the first factor is the relativistic kinetic energy denominator, and the second comes from the $m/E'$ factor in the $\tilde{v}_{\pi,\rm rel}$ [Eq. (2.9)]. The other $m/E$ factor in the $\tilde{v}_{\pi,\rm rel}$ operates on the $\Psi$. It is set to unity because most of the deuteron wave function has small relative momenta.

Neglecting the small difference between the relativistic and nonrelativistic $\Psi$, the ratio of the $\phi_D(p)$ is found to be

$$\frac{\phi_{D,\rm rel}(p)}{\phi_{D,\rm NR}(p)} = \frac{p^2}{2(\sqrt{m^2+p^2}-m)\sqrt{m^2+p^2}}. \tag{2.27}$$

The above estimate is fairly close to the ratio of the calculated *D*-wave functions as can be seen in Fig. 5. Note that this ratio is smaller if the $\tilde{v}_{\pi,\rm rel}$ is used with the nonrelativistic kinetic energy in $\phi_{D,\rm rel}(p)$ (dotted line), and it is larger than one when the $\tilde{v}_{\pi,\rm NR}$ is used with the relativistic kinetic energy (dot-dashed line). The relativistic corrections to the interaction and kinetic energies have opposite effects on the wave function. The difference between the *S*-wave functions is influenced by the changes in the kinetic energy and the $\tilde{v}_R$. The effects of these changes on the phase shifts and the deuteron energy must cancel by construction, and they seem to largely cancel in the $\phi_S(p)$.

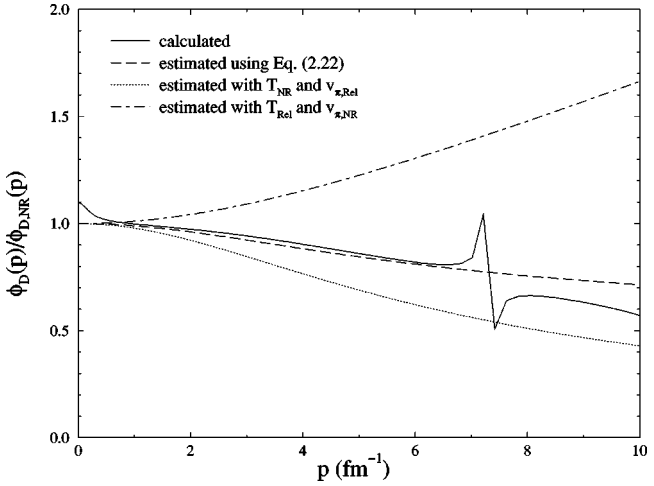


FIG. 5. Ratio of deuteron relativistic to nonrelativistic $D$-wave function in momentum space (solid line), and the simple estimate of Eq. (2.27) (dashed line). The dotted and dot-dashed lines represent results calculated using $T_{\rm NR}$, $\tilde{v}_{\pi,\rm rel}$ and $T_{\rm rel}$, $\tilde{v}_{\pi,\rm NR}$ in $\phi_{D,\rm rel}$ in Eq. (2.27), respectively. The wiggle in the calculated ratio around 7 fm$^{-1}$ comes from a node in the wave function.

Some of the deuteron momentum space results are listed in Table III. This table offers a microscopic view of how various relativistic effects were buried in the nonrelativistic models. Relativistic nonlocalities reduce the OPEP contribution by $\sim 2.6$ MeV, while the relativistic kinetic energy is smaller by $\sim -1$ MeV, giving a net effect of 1.6 MeV which is canceled by the change in the phenomenological $\tilde{v}_R$.

The variational Monte Carlo calculations for the $A>2$ systems have to be carried out in configuration space. We therefore have to Fourier transform the $\tilde{v}_{\pi,\rm rel}$ which depends on both $\mathbf{p}$ and $\mathbf{p}'$ [Eq. (2.9)], yielding a nonlocal potential in configuration space

$$\tilde{v}_{\pi,\rm rel}(\mathbf{r}',\mathbf{r})=\int \frac{d^3p}{(2\pi)^3}\frac{d^3p'}{(2\pi)^3}e^{-i\mathbf{p}'\cdot\mathbf{r}'}\tilde{v}_{\pi,\rm rel}(\mathbf{p}',\mathbf{p})e^{i\mathbf{p}\cdot\mathbf{r}}. \tag{2.28}$$

The exact integral in Eq. (2.28) is extremely difficult to calculate. The series obtained by expanding $\tilde{v}_{\pi,\rm rel}(\mathbf{p}',\mathbf{p})$ in powers of $p^2/m^2$ is given by

TABLE III. Results of momentum space deuteron calculations.

| | $\langle\Psi_{\rm NR}\vert H_{\rm NR}\vert\Psi_{\rm NR}\rangle$ | $\langle\Psi_R\vert H_R\vert\Psi_R\rangle$ |
|---|---|---|
| $\langle E\rangle$ | −2.242 | −2.242 |
| $\langle T\rangle$ | 19.882 | 18.877 |
| $\langle\tilde{v}_{ij}\rangle$ | −22.125 | −21.119 |
| $\langle\tilde{v}_\pi\rangle$ | −21.356 | −18.797 |
| $\langle\tilde{v}_R\rangle=\langle\tilde{v}_{ij}-\tilde{v}_\pi\rangle$ | −0.769 | −2.322 |
| $\langle\tilde{v}_{\pi,\rm rel}-\tilde{v}_{\pi,\rm NR}\rangle$ | | 2.589 |

$$\tilde{v}_{\pi,\rm rel}(\mathbf{p}',\mathbf{p})=\tilde{v}_{\pi,\rm NR}(\mathbf{q})\left(1-\frac{p^2+p'^2}{2m^2}+\frac{3p^4+2p^2p'^2+3p'^4}{8m^4}+\cdots\right). \tag{2.29}$$

However, this series does not have good convergence. In the case of deuteron, the expectation value of $\tilde{v}_{\pi,\rm NR}$, for the eigenfunction of our relativistic Hamiltonian is $-21.39$ MeV. The term in $\tilde{v}_{\pi,\rm rel}$, of order $1/m^2$, contributes 3.48 MeV to the $\langle\tilde{v}_{\pi,\rm rel}\rangle$, while that of order $1/m^4$ gives $-1.45$ MeV, and the exact $\langle\tilde{v}_{\pi,\rm rel}-\tilde{v}_{\pi,\rm NR}\rangle$ is 2.59 MeV. Therefore the series converges slowly to the exact value. This may appear surprising because the expectation value of the kinetic energy of the deuteron (Table III) is only about 20 MeV, giving $p^2/m^2\approx 0.02$ on average. However, the deuteron has large momentum components via the $D$ wave, or equivalently the tensor correlations, and most of the OPEP contribution is from those. Thus it is not surprising that the expectation value of OPEP is sensitive to higher powers of nucleon velocities.

For the relativistic OPEP, a good convergence is achieved by using the variables

$$\mathbf{Q}=\frac{1}{2}(\mathbf{p}+\mathbf{p}'),\quad \mathbf{q}=\mathbf{p}-\mathbf{p}', \tag{2.30}$$

$$\mathbf{x}=\frac{1}{2}(\mathbf{r}+\mathbf{r}'),\quad \mathbf{y}=\mathbf{r}-\mathbf{r}', \tag{2.31}$$

for which

$$\tilde{v}_{\pi,\rm rel}=\tilde{v}_{\pi,NR}(\mathbf{q})\frac{m^2}{\sqrt{(m^2+Q^2+q^2/4)^2-(\mathbf{Q}\cdot\mathbf{q})^2}},$$
$$=\tilde{v}_{\pi,\rm NR}(\mathbf{q})\left[1-\frac{Q^2+q^2/4}{m^2+Q^2+q^2/4}+\frac{1}{2}\frac{m^2(\mathbf{Q}\cdot\mathbf{q})^2}{(m^2+Q^2+q^2/4)^3}+\cdots\right]. \tag{2.32}$$

Here we expanded the $\tilde{v}_{\pi,\rm rel}$ in powers of $(\mathbf{Q}\cdot\mathbf{q})^2/(m^2+Q^2+q^2/4)^2$. This series appears to converge rapidly. In the case of deuteron, the leading relativistic correction given by the second term is 2.7 MeV, the third term gives $-0.18$ MeV, and the exact value is 2.59 MeV. The third term contains $\theta_{Qq}$ dependence and results in complicated operator forms as shown in the Appendix. Moreover, the third and higher terms account for only $\sim 4\%$ of the relativistic correction to OPEP expectation value in the deuteron (i.e., $\sim 0.6\%$ of $\langle\tilde{v}_{\pi,\rm rel}\rangle$). Therefore only the first two terms are considered in this work, and the relativistic OPEP is approximated by

$$\tilde{v}_{\pi,\rm rel}=\frac{m^2}{m^2+Q^2+q^2/4}\ \tilde{v}_{\pi,\rm NR}(\mathbf{q}). \tag{2.33}$$

With this $\tilde{v}_{\pi,\mathrm{rel}}$ in Eq. (2.14), we refit the phase shifts and deuteron binding energy. The parameters in $v_p(r)$ are very similar to those obtained with the exact $\tilde{v}_{\pi,\mathrm{rel}}$ given by Eq. (2.9). The new phase shifts and the relativistic potentials are very similar to those shown in Figs. 1 and 2.

The configuration space potential [Eq. (2.28)] is given by

$$\tilde{v}_{\pi,\mathrm{rel}}(\mathbf{x},\mathbf{y}) = \int \frac{d^3Q}{(2\pi)^3}\frac{d^3q}{(2\pi)^3}\frac{m^2}{m^2+Q^2+q^2/4} \times \tilde{v}_{\pi,\mathrm{NR}}(\mathbf{q}) e^{i(\mathbf{Q}\cdot\mathbf{y}+\mathbf{q}\cdot\mathbf{x})}, \tag{2.34}$$

and is simple to evaluate. The $\tilde{v}_{\pi,\mathrm{NR}}$ [Eq. (2.19)] in momentum space is given by

$$\tilde{v}_{\pi,\mathrm{NR}}(\mathbf{q}) = \int \tilde{v}_{\pi,\mathrm{NR}}(\mathbf{r}) e^{i\mathbf{q}\cdot\mathbf{r}} d^3r, = \frac{1}{3}\mu f_{\pi NN}^2 \left[ \mathcal{Y}_\pi(q)\boldsymbol{\sigma}_i\cdot\boldsymbol{\sigma}_j + \mathcal{T}_\pi(q) \times \left( \boldsymbol{\sigma}_i\cdot\boldsymbol{\sigma}_j - \frac{3}{q^2}\boldsymbol{\sigma}_i\cdot\mathbf{q}\boldsymbol{\sigma}_j\cdot\mathbf{q} \right) \right] \boldsymbol{\tau}_i\cdot\boldsymbol{\tau}_j, \tag{2.35}$$

where

$$\mathcal{Y}_\pi(q) = \int Y_\pi(r) j_0(qr) r^2 dr, \tag{2.36}$$

$$\mathcal{T}_\pi(q) = \int T_\pi(r) j_2(qr) r^2 dr. \tag{2.37}$$

Substituting these into Eq. (2.34) gives

$$\tilde{v}_{\pi,\mathrm{rel}}(x,y) = \frac{1}{3}\mu\frac{f_{\pi NN}^2}{4\pi} f(y)[F_{\sigma\tau}(x,y)\boldsymbol{\sigma}_i\cdot\boldsymbol{\sigma}_j + F_{t\tau}(x,y) S_{ij}(\hat{x},\hat{x})]\boldsymbol{\tau}_i\cdot\boldsymbol{\tau}_j, \tag{2.38}$$

with

$$F_{\sigma\tau}(x,y) = \frac{2}{\pi}\int q^2 dq \mathcal{Y}_\pi(q) j_0(qx) e^{-(\sqrt{m^2+q^2/4}-m)y}, \tag{2.39}$$

$$F_{t\tau}(x,y) = \frac{2}{\pi}\int q^2 dq \mathcal{T}_\pi(q) j_2(qx) e^{-(\sqrt{m^2+q^2/4}-m)y}, \tag{2.40}$$

$$f(y) = \frac{m^2}{4\pi}\frac{e^{-my}}{y}, \tag{2.41}$$

$$S_{ij}(\hat{x},\hat{x}) = 3\boldsymbol{\sigma}_i\cdot\hat{\mathbf{x}}\boldsymbol{\sigma}_j\cdot\hat{\mathbf{x}} - \boldsymbol{\sigma}_i\cdot\boldsymbol{\sigma}_j. \tag{2.42}$$

In the limit $m\to\infty$, $f(y)$ becomes $\delta^3(\mathbf{y})$, $F_{\sigma\tau}(x,y) \to Y_\pi(x)$, and $F_{t\tau}(x,y)\to T_\pi(x)$. When $\mathbf{y}\to 0$, we have $\mathbf{r}' = \mathbf{r}$, $\mathbf{x}=\mathbf{r}$ and Eq. (2.38) becomes $\tilde{v}_{\pi,\mathrm{NR}}$. Figure 6 shows $F_{\sigma\tau}(x,y)$ and $F_{t\tau}(x,y)$ as a function of $x$ for various values of $y$. Note that the solid lines for $y=0$ correspond to the nonrelativistic $Y_\pi(x)$ and $T_\pi(x)$. The volume integral of $F_{\sigma\tau}(x,y)$ is independent of $y$, whereas that of $F_{t\tau}(x,y)$ decreases with $y$. Therefore relativistic effects mostly come from the tensor part of OPEP.

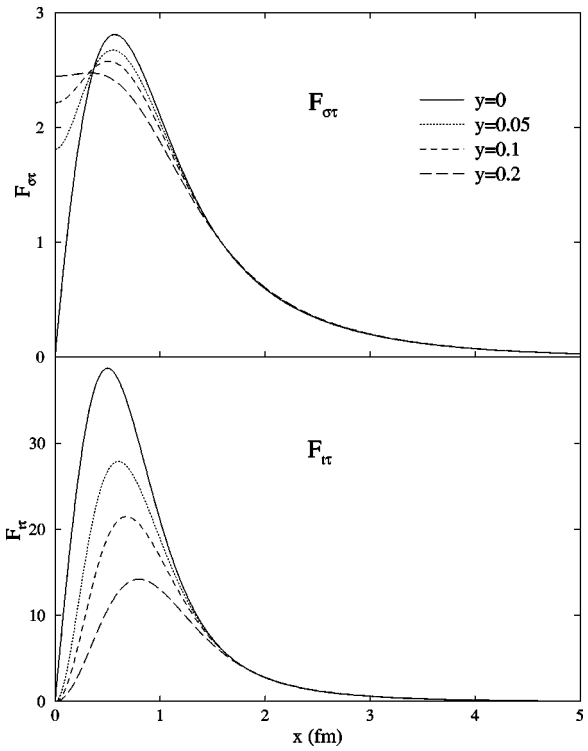


FIG. 6. $F_{\sigma\tau}$ and $F_{t\tau}$ as a function of $x$ for various values of $y$.

## III. VARIATIONAL MONTE CARLO CALCULATIONS AND RESULTS

### A. VMC techniques

With the relativistic Hamiltonian discussed in the previous section, we can proceed to evaluate the energy expectation value

$$\langle H_R\rangle = \langle T\rangle + \langle\tilde{v}_{ij}\rangle + \langle\delta v_{ij}\rangle + \langle\tilde{V}_{ijk}\rangle \tag{3.1}$$

for $A\geqslant 3$ nuclei using the Monte Carlo technique. The Monte Carlo method [31] offers a useful way to handle the multidimensional integrals which would otherwise be impractical by the usual numerical methods. The basis of this method is that instead of integrating over a regular array of points, we sum over a set of configurations $\{\mathbf{R}_i\}$ distributed with probability $w(\mathbf{R})$. Here $\mathbf{R}=(\mathbf{r}_1,\mathbf{r}_2,\ldots,\mathbf{r}_A)$ denotes the configuration of all the nucleons in the nucleus. There are various techniques for sampling $w(\mathbf{R})$ [31], and in this work Metropolis sampling method [32] is used to treat the complicated distributions.

The variational Monte Carlo (VMC) technique is based on variational principle that the minimum expectation value of the Hamiltonian is closest to the ground state energy of the system. Starting from a variational wave function, which depends upon several variational parameters

$(\alpha_1, \alpha_2, \ldots, \alpha_n)$, we evaluate the expectation value of the Hamiltonian using the Monte Carlo configuration samples $\mathbf{R}_i$:

$$\langle \hat{H} \rangle = \frac{\int d\mathbf{R} \Psi_v^\dagger(\mathbf{R}) \hat{H} \Psi_v(\mathbf{R})}{\int d\mathbf{R} \Psi_v^\dagger(\mathbf{R}) \Psi_v(\mathbf{R})} = \frac{(1/N_c) \sum_{i=1}^{N_c} [\Psi_v^\dagger(\mathbf{R}_i) \hat{H} \Psi_v(\mathbf{R}_i)]/w(\mathbf{R}_i)}{(1/N_c) \sum_{i=1}^{N_c} [\Psi_v^\dagger(\mathbf{R}_i) \Psi_v(\mathbf{R}_i)]/w(\mathbf{R}_i)} \pm \delta, \tag{3.2}$$

where $\delta$ is the standard deviation. Typically block averaging scheme is used to obtain a normal distribution and the error can be conveniently evaluated from it. We divide $N_c$ configurations into $N_b$ blocks each containing $N_0 = N_c / N_b$ configurations. The average

$$\tilde{H}_b = \frac{(1/N_0) \sum_{i=1}^{N_0} [\Psi_v^\dagger(\mathbf{R}\_i) \hat{H} \Psi_v(\mathbf{R}_i)]/w(\mathbf{R}_i)}{(1/N_0) \sum_{i=1}^{N_0} [\Psi_v^\dagger(\mathbf{R}_i) \Psi_v(\mathbf{R}_i)]/w(\mathbf{R}_i)} \tag{3.3}$$

is evaluated for each block. The expectation value of $H$ is given by

$$\langle H \rangle = \frac{1}{N_b} \sum_{i=1}^{N_b} \tilde{H}_b \tag{3.4}$$

with the standard deviation

$$\delta = \frac{1}{N_b} \sqrt{\sum_{i=1}^{N_b} (\tilde{H}_b - \langle H \rangle)^2}. \tag{3.5}$$

The Monte Carlo result is exact when the number of configurations $N_c \to \infty$, although in practice $N_c = 50\,000$ seems to be enough to obtain results with sufficiently small statistical errors. The weight function is usually chosen to be

$$w(\mathbf{R}_i) = \Psi_v^\dagger(\mathbf{R}_i) \Psi_v(\mathbf{R}_i) \tag{3.6}$$

to maintain small Monte Carlo error. Note that when $\Psi_v$ is the eigenstate of $H$, the Monte Carlo sampling error becomes zero. Finally, the parameters $(\alpha_1, \alpha_2, \ldots, \alpha_n)$ are varied to minimize the energy.

Some of the terms in $\langle H_R \rangle$ [Eq. (3.1)] can be calculated straightforwardly and have been discussed in Refs. [33] and [13]. The terms that require special techniques are the relativistic kinetic energy $\langle \sqrt{m^2 - \nabla^2} \rangle$ and $\tilde{v}_{\pi,\mathrm{rel}}$ in the two-body potential. The kinetic energy term has been calculated previously in Ref. [12], and the calculation of $\langle \tilde{v}_{\pi,\mathrm{rel}} \rangle$ is discussed in Sec. III C.

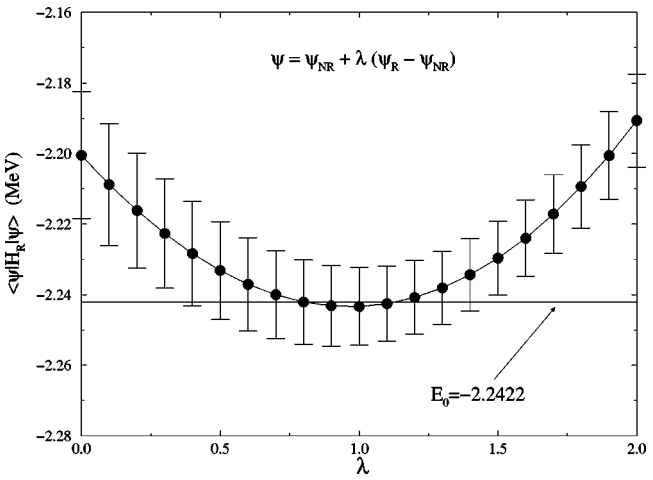


FIG. 7. VMC results for deuteron with 100 000 configurations.

### B. Relativistic wave functions

In the nonrelativistic case, variational wave functions of the form

$$|\Psi_v\rangle = \left(1 + \sum_{i<j<k} F_{ijk}\right) \left(\mathcal{S} \prod_{i<j} F_{ij}\right) |\Phi\rangle, \tag{3.7}$$

having symmetrized product of pair correlation operators $F_{ij}$ and a sum of triplet correlations $F_{ijk}$ operating on an antisymmetric, uncorrelated wave function $|\Phi\rangle$, have been commonly used. The $F_{ij}$ and $F_{ijk}$ correlation operators reflect the effects of two-, three-body interactions on the wave function. The uncorrelated wave function has no spatial dependence for $A \leqslant 4$ nuclei. A good representation of such a wave function is given in Ref. [33].

The pair correlation operator $F_{ij}$ is constructed from correlation functions which satisfy Schrödinger-like two-body equations, with appropriate boundary conditions. Their solutions are similar to deuteron wave functions $\Psi_{\mathrm{NR}}$ and $\Psi_R$ displayed in Fig. 3. In the case of $A = 2$ deuteron, both nonrelativistic and relativistic correlation functions can be easily solved in momentum space; they are not very different from each other as can be seen in Fig. 3. In $A > 2$ nuclei, the nonrelativistic pair correlation equations can be easily solved in configurations space, however, the relativistic equations are more difficult to solve. Therefore we seek good approximations for the relativistic pair correlation functions.

Our method can be easily illustrated using the example of deuteron. Its variational wave function is expressed as

$$\Psi = \Psi_{\mathrm{NR}} + \lambda (\Psi_R - \Psi_{\mathrm{NR}}), \tag{3.8}$$

$\langle \Psi | H_R | \Psi \rangle$ is calculated using VMC, and $\lambda$ is varied to minimize it. The results are shown in Fig. 7. The error bars shown in Fig. 7 originate from the statistical sampling and are $< 1\%$ of the binding energy. The same configurations are used to calculate the energies for all $\lambda$, hence the errors are correlated. The minimum value of $\langle H_R \rangle$ does occur at $\lambda = 1$ where $\Psi = \Psi_R$ as expected. The difference in $\langle H_R \rangle$ between $\lambda = 0$ (using a nonrelativistic wave function) and $\lambda = 1$ (using a relativistic one) is $\sim 0.04$ MeV. This means

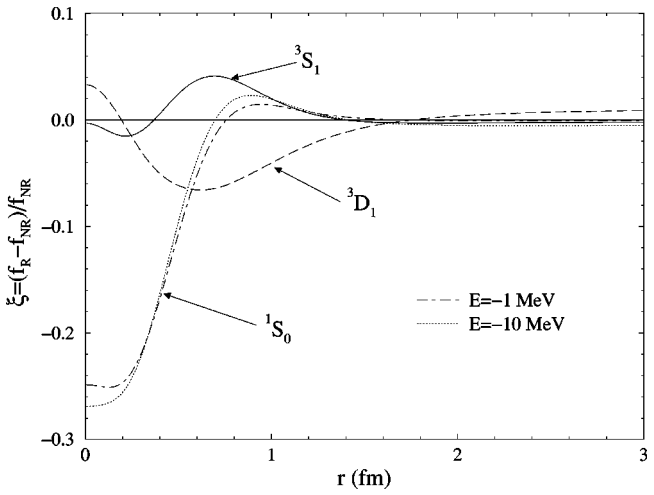


FIG. 8. $\xi=(f_R-f_{\rm NR})/f_{\rm NR}$ as a function of $r$.

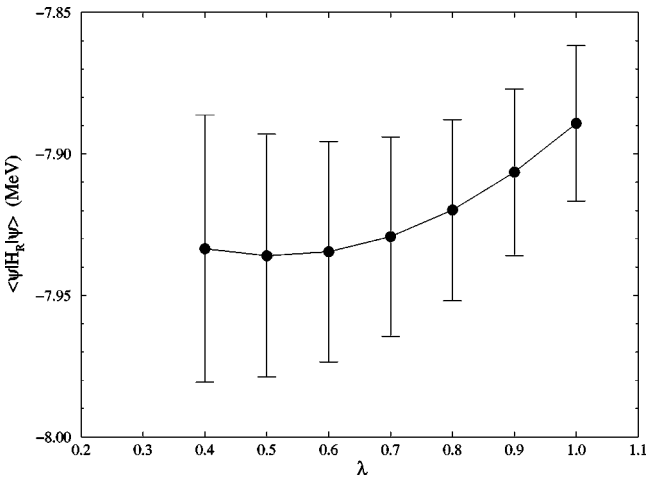


FIG. 9. VMC results for triton with 50 000 configurations.

that if we were to use the nonrelativistic wave function to calculate the expectation value of $H_R$, the result will be off by only 2% for the deuteron.

In heavier nuclei we also expect the optimum nonrelativistic wave function to provide a good approximation for relativistic wave function. The difference between the two is presumably largest in ${}^3S_1-{}^3D_1$ and ${}^1S_0$ correlation functions at small $r$. We therefore define

$$f^c_{0,1}=f^c_{0,1,\rm NR}(1+\lambda\xi_{{}^1S_0}), \tag{3.9}$$

$$f^c_{1,0}=f^c_{1,0,\rm NR}(1+\lambda\xi_{{}^3S_1}), \tag{3.10}$$

$$f^t_{1,0}=f^t_{1,0,\rm NR}(1+\lambda\xi_{{}^3D_1}), \tag{3.11}$$

where $\xi_c$ for the channel $c$ is defined as

$$\xi_c(r)=\frac{\phi_{c,R}(r)-\phi_{c,\rm NR}(r)}{\phi_{c,\rm NR}(r)}. \tag{3.12}$$

At small $r$, the central $f^c_{1,0}$ and tensor $f^t_{1,0}$ correlation functions in spin-isospin $S,T=1,0$ states are proportional to the $S$ and $D$ radial wave functions of the deuteron, respectively. Therefore the $\xi_{{}^3S_1}$ and $\xi_{{}^3D_1}$ can be calculated exactly in momentum space using the relativistic and nonrelativistic deuteron wave functions for the $\phi_{c,R}$ and $\phi_{c,\rm NR}$. These $\xi$'s are rather short ranged (Fig. 8), and we do not expect them to vary significantly in larger nuclei. Wiringa [4] has shown that the nonrelativistic correlation functions for ${}^2$H, ${}^3$H, and ${}^4$He are almost the same at small $r$.

A similar calculation of $\xi_{{}^1S_0}$ is not possible because of the absence of a bound state in that channel. However, we can obtain an artificial ${}^1S_0$ bound state by slightly increasing the strength of intermediate range attraction in $v({}^1S_0)$. The binding energy and the wave function at large $r$ are very sensitive to small changes in $v({}^1S_0)$, however, $\xi_{{}^1S_0}$ is relatively insensitive. As an example, the $\xi_{{}^1S_0}$ obtained from artificial ${}^1S_0$ bound states with energies of $-1$ and $-10$ MeV, shown in Fig. 8, are very similar.

The VMC energy of ${}^3$H with the relativistic Hamiltonian is shown as a function of $\lambda$ in Fig. 9. The minimum occurs at $\lambda=0.5$ instead of 1 (the expected value), however, the difference in $\langle H_R\rangle$ between $\lambda=0.5$ and 1 is rather small and of the order of the Monte Carlo sampling error. The minimum energy for ${}^4$He occurs at the expected $\lambda=1.0$.

### C. Expectation value of the nonlocal potential

Consider an $A$-nucleon system whose wave function is denoted as $\Psi(\mathbf{r}_1,\mathbf{r}_2,\ldots,\mathbf{r}_A)$. We define

$$\mathbf{x}_i=\frac{1}{2}(\mathbf{r}_i+\mathbf{r}'_i),\quad \mathbf{x}_j=\frac{1}{2}(\mathbf{r}_j+\mathbf{r}'_j), \tag{3.13}$$

so that

$$\mathbf{x}=\mathbf{x}_i-\mathbf{x}_j,\quad \frac{\mathbf{y}}{2}=\mathbf{r}_i-\mathbf{r}'_i=\mathbf{r}'_j-\mathbf{r}_j, \tag{3.14}$$

as illustrated in Fig. 10. The expectation value of relativistic OPEP is then given by

$$\begin{aligned}\langle\tilde{v}_{\pi,\rm rel}\rangle=&\sum_{i<j}\int\prod_{k\neq i,j}d^3r_k d^3x_i d^3x_j d^3y\\ &\times\Psi^\dagger\left(\mathbf{r}_1,\ldots,\mathbf{x}_i-\frac{\mathbf{y}}{4},\ldots,\mathbf{x}_j+\frac{\mathbf{y}}{4},\ldots,\mathbf{r}_A\right)\\ &\times\tilde{v}_{\pi,\rm rel}(|\mathbf{x}_i-\mathbf{x}_j|,y)\\ &\times\Psi\left(\mathbf{r}_1,\ldots,\mathbf{x}_i+\frac{\mathbf{y}}{4},\ldots,\mathbf{x}_j-\frac{\mathbf{y}}{4},\ldots,\mathbf{r}_A\right),\end{aligned} \tag{3.15}$$

where $\tilde{v}_{\pi,\rm rel}(|\mathbf{x}_i-\mathbf{x}_j|,y)$ is previously calculated in Eq. (2.38). The integration over the $\mathbf{r}_k$'s, $\mathbf{x}_i$, $\mathbf{x}_j$ and the solid angle of $\mathbf{y}$ is carried out by the Monte Carlo method, while that over the magnitude of $y$ is carried out with Gauss-Laguerre integral.

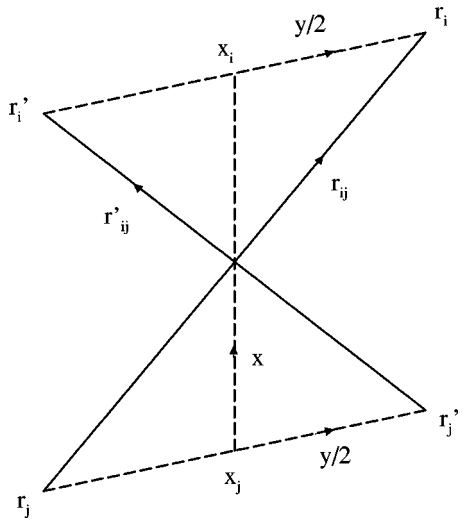


FIG. 10. A diagram to illustrate the calculation of nonlocal interaction contributions.

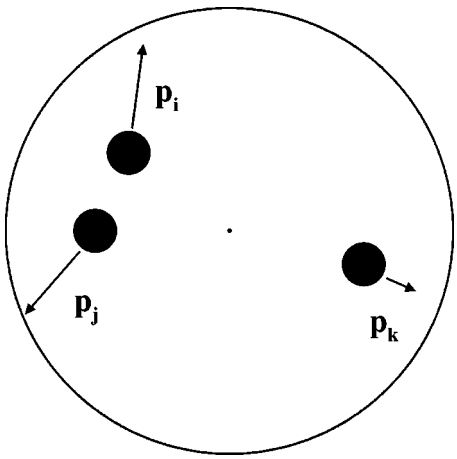


FIG. 11. A naive picture of $^3$H to illustrate large momentum contribution from a configuration where two nucleons are close together.

### D. VMC results

The VMC results for $^3$H and $^4$He are listed in Table IV. Note that in principle we should use GFMC to calculate the exact binding energies, but the relativistic effects resulting from the difference between $\langle H_R\rangle$ and $\langle H_{\rm NR}\rangle$ are small and presumably not too different from those estimated using VMC.

The total relativistic effect on the binding energy is $\sim 0.3$ MeV for $^3$H and $\sim 1.8$ MeV for $^4$He. Most of the effect comes from the boost correction which is 0.42 MeV for $^3$H and 1.94 MeV for $^4$He. The net effect of relativistic corrections to the kinetic energy and the two-body potential, on the binding energy is rather small: $\sim -0.12 \pm 0.06$ MeV in ($^3$H) and $\sim -0.17 \pm 0.10$ MeV in ($^4$He). Since both $H_{\rm NR}$ and $H_R$ are constrained to give the same deuteron binding energy, the changes in $\langle T\rangle$ and $\langle \tilde{v}_{ij}\rangle$ cancel exactly in $^2$H. In $^3$H and $^4$He they appear to largely cancel and give a rather small net effect.

In view of the slow convergence of the $\langle|\tilde{v}_{\pi,\rm rel}-\tilde{v}_{\pi,\rm NR}|\rangle$, when expanded in powers of $p^2/m^2$, one may question the validity of calculating the boost interaction $\delta v$ only up to first order in $P^2/4m^2$. The average kinetic energies of nucleons in nuclei are rather small giving average $p_i^2/m^2 < 0.1$. The expansion has good convergence for such values. However, two nucleons can occasionally have large relative momenta when they come close together as illustrated in Fig. 11. In that configuration $\mathbf{p}_i \sim \mathbf{p}$ and $\mathbf{p}_j \sim -\mathbf{p}$ are both large due to strong short-range interaction between nucleons $i$ and $j$. Such configurations are responsible for the slow convergence of the expansion of $\langle|\tilde{v}_{\pi,\rm rel}-\tilde{v}_{\pi,\rm NR}|\rangle$. In these configurations the squares of the total pair momenta are of order $P_{ik}^2 \sim P_{jk}^2 \sim p^2$, while $P_{ij}^2$ has small, near average value. Thus the expansion parameter $P^2/4m^2$ for the boost interaction is effectively four times smaller than that of $(\tilde{v}_{\pi,\rm rel}-\tilde{v}_{\pi,\rm NR})$ when the momenta are generated by pair correlations, therefore we expect the boost expansion to converge more rapidly. Moreover, $\langle|\tilde{v}_{\pi,\rm rel}-\tilde{v}_{\pi,\rm NR}|\rangle$ is much larger ($\sim 6$ and 13 MeV in $^3$H and $^4$He, respectively) than $\langle|\delta v|\rangle$ and has to be calculated with higher relative accuracy to obtain a final total energy with error $\sim 1\%$.

## IV. CONCLUSIONS AND OUTLOOK

We find that the relativistic effects in OPEP are quite substantial. The expectation values of $\tilde{v}_{\pi,\rm rel}$ are smaller than

TABLE IV. VMC results for $^3$H and $^4$He, calculated with 50 000 configurations.

| | $^3$H | | | $^4$He | | |
|---|---|---|---|---|---|---|
| | $H_{\rm NR}$ | $H_R$ | $H_R-H_{\rm NR}$ | $H_{\rm NR}$ | $H_R$ | $H_R-H_{\rm NR}$ |
| $\langle E\rangle$ [a] | −8.24(3) | −7.94(4) | 0.30(5) | −28.09(7) | −26.32(8) | 1.8(1) |
| $\langle T\rangle$ | 50.1(5) | 48.6(5) | −1.5(7) | 104.8(9) | 98.4(8) | −6(1) |
| $\langle \tilde{v}_{ij}\rangle$ | −57.3(5) | −56.0(5) | 1.3(7) | −127.6(9) | −121.5(9) | 6(1) |
| $\langle \tilde{V}_{ijk}\rangle$ | −1.06(3) | −1.03(3) | | −5.29(9) | −5.20(8) | |
| $\langle \delta v_{ij}\rangle$ | | 0.42(1) | | | 1.94(3) | |
| $\langle \tilde{V}^R_{ijk}\rangle$ | 0.98(3) | 1.01(3) | | 5.26(7) | 5.38(8) | |
| $\langle \tilde{v}_\pi\rangle$ | −44.0(2) | −38.3(2) | 5.7(4) | −97.1(5) | −83.8(4) | 13.3(1) |

[a]Without electromagnetic interaction.

those of $\tilde{v}_{\pi,\mathrm{NR}}$ by $\sim 15\%$. Since the expectation values of OPEP are much larger than nuclear binding energies, the differences in the OPEP expectation values are comparable to the total nuclear energy. However, nuclear Hamiltonians are not derived from first principles, they are obtained by fitting data. The substantial difference between $\tilde{v}_{\pi,\mathrm{rel}}$ and $\tilde{v}_{\pi,\mathrm{NR}}$ is compensated in the $H_{\mathrm{NR}}$ by that in the kinetic energy $T$ and $\tilde{v}_R$ so that $H_{\mathrm{NR}}$ gives the same scattering cross sections and deuteron energy as the $H_R$. We find that this compensation works rather well for three- and four-body nuclei. In absence of the boost interaction our nonrelativistic and relativistic Hamiltonians seem to give very similar results for the binding energies and wave functions of light nuclei. It is probably necessary to examine one-pion exchange current contributions to elastic scattering form factors and radiative capture reactions to see the effect of the $m/E$ factors in the OPEP.

The modern two-nucleon potential models, which include the Nijmegen models I, II, and Reid-93 [34], Argonne $v_{18}$ [6], and CD-Bonn [25], accurately reproduce the $NN$-scattering data in the Nijmegen data base. Friar *et al.* [35] have studied the triton energy with the Nijmegen and Argonne models, without boost or three-nucleon interactions, using accurate Faddeev calculations. The energies obtained with the three local potential models, Reid-93, Nijmegen-II, and Argonne $v_{18}$ are, respectively, $-7.63$, $-7.62$, and $-7.61$ MeV. These energies are very close, and these models also give very similar values (5.70, 5.64, and 5.76 %) for $P_D$, the fraction of $D$ state in the deuteron. The boson exchange Nijmegen-I model contains nonlocal terms and gives $-7.72$ MeV for triton energy and 5.66% for $P_D$. Comparison of the results of Nijmegen I and II models indicates that the total effect of the nonlocalities on energies and the wave functions could be small. The present results support this conclusion; inclusion of relativistic nonlocalities in OPEP and kinetic energy lowers the triton energy by $\sim 0.1$ MeV and $P_D$ by 0.04%.

In contrast the CD-Bonn potential gives rather different results from the Nijmegen and Argonne models. It gives a triton energy of $-8.00$ MeV and $P_D = 4.83\%$. The deuteron wave functions predicted by the five modern $NN$-interaction models are compared in Ref. [36]. The CD-Bonn $D$-state wave function is smaller at intermediate distances than those of the other models. The OPEP in the CD-Bonn model [Eq. (2.10)], has additional off-shell nonlocalities predicted by pseudoscalar pion-nucleon coupling. It is interesting to note that the difference in the OPEP is the main cause of the difference between CD-Bonn and the other models. A potential containing $\tilde{v}_{\pi,\mathrm{CDB}}$ and $\tilde{v}_R$ parametrized as in Argonne $v_{18}$, re-tuned to fit the scattering data, gives a smaller $D$ state with $P_D = 4.98\%$ [37]. After choosing the OPEP, the shorter ranged parts of the nuclear forces seem to be better constrained by the data. Perhaps, the correct form of OPEP can be derived from chiral perturbation theory or QCD. The $V_{ijk}$ also depends upon the choice of OPEP, however, Coon and Friar have argued that the final observables should not depend up on that choice [27].

The boost interaction $\delta v$ gives the dominant relativistic correction to the binding energies of light nuclei in the present formalism. Contributions of $\delta v$ are very small, only $\sim 1\%$ of that of $\tilde{v}$ in $^3$H and $^4$He. However they are not canceled, since $H_{NR}$ does not have this term, and therefore dominate the net effect. As with the two-nucleon interaction, the three-nucleon interaction is also not derived from first principles. Urbana models of $V_{ijk}$ contain two terms: the attractive two-pion exchange term $V_{ijk}^{2\pi}$ and a repulsive phenomenological term $V_{ijk}^{R}$. Their strengths are chosen to reproduce the triton energy and the density of nuclear matter without considering any relativistic effects. In light nuclei the repulsive $\delta v$ contribution is about 37% of that of $V_{ijk}^{R}$. Thus the strength of $V_{ijk}^{R}$ in $H_R$ has to be reduced by 37% to obtain the experimental energies of light nuclei. The difference in the three nucleon interaction then compensates for the omission of $\delta v$ in conventional nonrelativistic nuclear Hamiltonians. It appears that this compensation works rather well in light nuclei having up to eight nucleons [38], as well as in nuclear and neutron matter up to normal densities [39]. However, at several times nuclear matter densities, encountered in neutron stars, the effective three-nucleon interaction overestimates the $\delta v$ contribution significantly [39].

The energies and the wave functions predicted by the nonrelativistic Hamiltonian [Eq. (1.1)] seem to be little changed by including the relativistic effects studied in this work, provided the interactions $v_{ij}$ and $V_{ijk}$ are obtained from accurate fits to the scattering data, triton energy and nuclear matter density. We have not studied all the relativistic effects in nuclei. There are presumably many more buried in the phenomenological $\tilde{v}$. However, the pair distribution functions at small $r$ do not change from nucleus to nucleus [40]. Therefore the deuteron provides an excellent test of the $NN$ wave function at small $r$ in nuclei. The recently completed experiments at Jefferson Lab [41] show that the deuteron form factors are in reasonable agreement with the predictions of the Argonne $v_{18}$ model [6] up to momentum transfer of two GeV. It thus appears unlikely that the wave functions predicted by $H_{\mathrm{NR}}$ are significantly wrong at distances larger than $\sim 0.5$ fm.

## ACKNOWLEDGMENTS

The authors would like to thank J. Carlson and R. Schiavilla for many interesting discussions and R. B. Wiringa for his help on the nonrelativistic variational wave function. A.A. acknowledges the kind hospitality of the Physics Department of the University of Illinois at Urbana-Champaign, where a large part of this work was performed. The calculations were performed on IBM SP machines at Cornell Theory Center, and on Cray supercomputers at Pittsburgh Supercomputing Center. This work was supported by the U.S. National Science Foundation under Grant No. PHY94-21309, and the work of A.A. by Universidade de Lisboa, Junta de Investigação Cientí fica e Tecnológica under Contract No. PBIC/C/CEN/1108/92.

## APPENDIX: RELATIVISTIC OPEP IN CONFIGURATION SPACE

The third term in Eq. (2.32) gives the second-order relativistic correction to OPEP and is denoted as $v^{(2)}$:

$$v^{(2)}(\mathbf{x},\mathbf{y})=\int \frac{d^3Q}{(2\pi)^3}\frac{d^3q}{(2\pi)^3}g(q,Q) \times\cos^2\theta_{qQ}\tilde{v}_{\pi,\mathrm{NR}}(\mathbf{q})e^{i(\mathbf{Q}\cdot\mathbf{y}+\mathbf{q}\cdot\mathbf{x})}, \quad \text{(A1)}$$

where $\theta_{qQ}$ is the angle between $\mathbf{q}$ and $\mathbf{Q}$, and

$$g(q,Q)=\frac{1}{2}\frac{m^2Q^2q^2}{(m^2+Q^2+q^2/4)^3}. \quad \text{(A2)}$$

Expressing $\cos^2\theta_{qQ}$ as

$$\cos^2\theta_{qQ}=\frac{2}{3}P_2(\cos\theta_{qQ})+\frac{1}{3}, \quad \text{(A3)}$$

we get

$$v^{(2)}(\mathbf{x},\mathbf{y})=\frac{1}{3}\int \frac{d^3Q}{(2\pi)^3}\frac{d^3q}{(2\pi)^3}g(q,Q) \times\tilde{v}_{\pi,\mathrm{NR}}(\mathbf{q})e^{i(\mathbf{Q}\cdot\mathbf{y}+\mathbf{q}\cdot\mathbf{x})} +\frac{2}{3}\int \frac{d^3Q}{(2\pi)^3}\frac{d^3q}{(2\pi)^3}g(q,Q) \times P_2(\cos\theta_{qQ})\tilde{v}_{\pi,\mathrm{NR}}(\mathbf{q})e^{i(\mathbf{Q}\cdot\mathbf{y}+\mathbf{q}\cdot\mathbf{x})}. \quad \text{(A4)}$$

The first integral denoted by $v_1^{(2)}(\mathbf{x},\mathbf{y})$ is independent of $\theta_{qQ}$ and can be easily evaluated by using Eq. (2.35) and the following identities:

$$e^{i\mathbf{q}\cdot\mathbf{r}}=4\pi\sum_{lm} i^l Y_{lm}^*(\hat{q})Y_{lm}(\hat{r})j_l(qr), \quad \text{(A5)}$$

$$\int Y_{lm}^*(\hat{q})Y_{l'm'}(\hat{q})d\Omega_q=\delta_{ll'}\delta_{mm'}, \quad \text{(A6)}$$

$$\int v(r)\boldsymbol{\sigma}_i\cdot\hat{r}\boldsymbol{\sigma}_j\cdot\hat{r}e^{i\mathbf{q}\cdot\mathbf{r}}d^3r =-\boldsymbol{\sigma}_i\cdot\boldsymbol{\nabla}_q\boldsymbol{\sigma}_j\cdot\boldsymbol{\nabla}_q\int v(r)e^{i\mathbf{q}\cdot\mathbf{r}}\frac{1}{r^2}d^3r. \quad \text{(A7)}$$

We obtain

$$v_1^{(2)}(\mathbf{x},\mathbf{y})=\frac{\mu}{9\pi^3}\frac{f_{\pi NN}^2}{4\pi} \times\Big[\int Q^2dQq^2dqg(q,Q) \times\mathcal{Y}_\pi(q)j_0(Qy)j_0(qx)\boldsymbol{\sigma}_i\cdot\boldsymbol{\sigma}_j +\int Q^2dQq^2dqg(q,Q)\mathcal{T}_\pi(q) \times j_0(Qy)j_2(qx)S_{ij}(\hat{x},\hat{x})\Big]\boldsymbol{\tau}_i\cdot\boldsymbol{\tau}_j, \quad \text{(A8)}$$

where $\mathcal{Y}_\pi(q)$ and $\mathcal{T}_\pi(q)$ were previously given in Eqs. (2.36) and (2.37).

To calculate the second integral in Eq. (A4), we use

$$P_l(\cos\theta_{qQ})=\frac{4\pi}{2l+1}\sum_m Y_{lm}^*(\hat{Q})Y_{lm}(\hat{q}). \quad \text{(A9)}$$

The integral over the solid angles becomes

$$\int d\Omega_Q d\Omega_q e^{i(\mathbf{Q}\cdot\mathbf{y}+\mathbf{q}\cdot\mathbf{x})}P_2(\cos\theta_{qQ}) =(4\pi)^2P_2(\cos\theta_{xy})j_2(Qy)j_2(qx) \quad \text{(A10)}$$

and the second term in Eq. (A4), denoted by $v_2^{(2)}(\mathbf{x},\mathbf{y})$, is

$$v_2^{(2)}(\mathbf{x},\mathbf{y})=\frac{2\mu}{9\pi^3}\frac{f_{\pi NN}^2}{4\pi}\Big\{P_2(\cos\theta_{xy})\int Q^2dQq^2dqg(q,Q) \times[\mathcal{Y}_\pi(q)+\mathcal{T}_\pi(q)]j_2(Qy)j_2(qx)\boldsymbol{\sigma}_i\cdot\boldsymbol{\sigma}_j, +3\boldsymbol{\sigma}_i\cdot\boldsymbol{\nabla}_x\boldsymbol{\sigma}_j\cdot\boldsymbol{\nabla}_x\Big[P_2(\cos\theta_{xy}) \times\int Q^2dQdqg(q,Q)\mathcal{T}_\pi(q)j_2(Qy)j_2(qx)\Big]\Big\} \times\boldsymbol{\tau}_i\cdot\boldsymbol{\tau}_j. \quad \text{(A11)}$$

Here $\theta_{xy}$ is the angle between $\mathbf{x}$ and $\mathbf{y}$. The gradient operators $\boldsymbol{\nabla}_x$ in the second term act on both $P_2(\cos\theta_{xy})$ and $j_2(qx)$.

The $Q$ integral in Eqs. (A8) and (A11) can be performed analytically and results in

$$\int Q^2dQg(q,Q)j_0(Qy)=f(y)[Z_2(q,y)-Z_1(q,y)], \quad \text{(A12)}$$

$$\int Q^2dQg(q,Q)j_2(Qy)=f(y)Z_1(q,y), \quad \text{(A13)}$$

where $f(y)$ is the Yukawa function given in Eq. (2.33) and

$$Z_1(q,y)=\frac{(\pi qy)^2}{8}\exp\Big[-\Big(\sqrt{m^2+\frac{q^2}{4}}-m\Big)y\Big], \quad \text{(A14)}$$

$$Z_2(q,y)=\frac{3}{\sqrt{m^2+(q^2/4)}y}Z_1(q,y). \quad \text{(A15)}$$

$v^{(2)}$ is finally obtained as

$$v^{(2)}(\mathbf{x},\mathbf{y})=\frac{\mu}{3}\frac{f_{\pi NN}^2}{4\pi}f(y)[I_1(x,y,\theta_{xy})\boldsymbol{\sigma}_i\cdot\boldsymbol{\sigma}_j +I_2(x,y,\theta_{xy})S_{ij}(\hat{x},\hat{x})+I_3(x,y,\theta_{xy})S_{ij}(\hat{y},\hat{y}) +I_4(x,y,\theta_{xy})S_{ij}(\hat{x},\hat{y})]\boldsymbol{\tau}_i\cdot\boldsymbol{\tau}_j, \quad \text{(A16)}$$

where the tensor operator $S_{ij}(\hat{x},\hat{y})$ is defined as

$$S_{ij}(\hat{x},\hat{y}) = \frac{3}{2}(\boldsymbol{\sigma}_i\cdot\hat{x}\,\boldsymbol{\sigma}_j\cdot\hat{y} + \boldsymbol{\sigma}_i\cdot\hat{y}\,\boldsymbol{\sigma}_j\cdot\hat{x}) - \hat{x}\cdot\hat{y}\,\boldsymbol{\sigma}_i\cdot\boldsymbol{\sigma}_j, \tag{A17}$$

and $I_1$, $I_2$, $I_3$, and $I_4$ are given by

$$I_1(x,y,\theta_{xy}) = \mathcal{F}^{\mathcal{Y}}_{20}(x,y) - \mathcal{F}^{\mathcal{Y}}_{10}(x,y) + 2\mathcal{F}^{\mathcal{Y}}_{12}(x,y)P_2(\cos\theta_{xy}), \tag{A18}$$

$$I_2(x,y,\theta_{xy}) = \mathcal{F}^{\mathcal{T}}_{22}(x,y) - 3\mathcal{H}^{\mathcal{T}}_{13}(x,y) + 3\mathcal{F}^{\mathcal{T}}_{14}(x,y)\cos^2\theta_{xy}, \tag{A19}$$

$$I_3(x,y,\theta_{xy}) = 6\mathcal{H}^{\mathcal{T}}_{12}(x,y), \tag{A20}$$

$$I_4(x,y,\theta_{xy}) = -12\mathcal{H}^{\mathcal{T}}_{13}(x,y)\cos\theta_{xy}, \tag{A21}$$

where

$$\mathcal{F}^{\mathcal{Y}}_{\alpha l}(x,y) = \frac{1}{3\pi^3}\int q^2 dq Z_\alpha(q,y)\mathcal{Y}_\pi(q) j_l(qx), \tag{A22}$$

$$\mathcal{F}^{\mathcal{T}}_{\alpha l}(x,y) = \frac{1}{3\pi^3}\int q^2 dq Z_\alpha(q,y)\mathcal{T}_\pi(q) j_l(qx), \tag{A23}$$

$$\mathcal{H}^{\mathcal{T}}_{\alpha l}(x,y) = \frac{1}{3\pi^3}\int q^2 dq Z_\alpha(q,y)\mathcal{T}_\pi(q)\frac{j_l(qx)}{(qx)^{4-l}}. \tag{A24}$$


[1] W. Glöckle and H. Kamada, Phys. Rev. Lett. **71**, 971 (1993).
[2] A. Kievsky, M. Viviani, and S. Rosati, Nucl. Phys. **A551**, 241 (1993); **A577**, 511 (1994).
[3] J. Carlson, in *Structure of Hadrons and Hadronic Matter*, edited by O. Scholten and J. H. Koch (World Scientific, Singapore, 1991), p. 43.
[4] R. B. Wiringa, Phys. Rev. C **43**, 1585 (1991).
[5] B. S. Pudliner, V. R. Pandharipande, J. Carlson, and R. B. Wiringa, Phys. Rev. Lett. **74**, 4396 (1995); B. S. Pudliner, V. R. Pandharipande, J. Carlson, Steven C. Pieper, and R. B. Wiringa, Phys. Rev. C **56**, 1720 (1997).
[6] R. B. Wiringa, V. G. J. Stoks, and R. Schiavilla, Phys. Rev. C **51**, 38 (1995); **54**, 646 (1996).
[7] S. C. Pieper (private communication).
[8] G. Rupp and J. A. Tjon, Phys. Rev. C **45**, 2133 (1992).
[9] F. Sammarruca and R. Machleidt, Few Body Syst. **24**, 87 (1998).
[10] Alfred Stadler and Franz Gross, Phys. Rev. Lett. **78**, 26 (1997).
[11] B. D. Keister and W. N. Polyzou, Adv. Nucl. Phys. **20**, 225 (1991).
[12] J. Carlson, V. R. Pandharipande, and R. Schiavilla, Phys. Rev. C **47**, 484 (1993).
[13] J. L. Forest, V. R. Pandharipande, J. Carlson, and R. Schiavilla, Phys. Rev. C **52**, 576 (1995).
[14] B. Bakamjian and L. H. Thomas, Phys. Rev. **92**, 1300 (1952).
[15] L. L. Foldy, Phys. Rev. **122**, 275 (1961).
[16] R. A. Krajcik and L. L. Foldy, Phys. Rev. D **10**, 1777 (1974).
[17] J. L. Friar, Phys. Rev. C **12**, 695 (1975).
[18] J. L. Forest, V. R. Pandharipande, and J. L. Friar, Phys. Rev. C **52**, 568 (1995).
[19] H. A. Bethe and E. E. Salpeter, *Quantum Mechanics of One and Two Electron Atoms* (Academic Press, New York, 1957).
[20] F. Coester, S. C. Pieper, and F. J. D. Serduke, Phys. Rev. C **11**, 1 (1974).
[21] W. Glöckle, T.-S.H. Lee, and F. Coester, Phys. Rev. C **33**, 709 (1986).
[22] B. D. Serot and J. D. Walecka, Adv. Nucl. Phys. **16**, 1 (1986).
[23] J. L. Friar, Phys. Rev. C **22**, 796 (1980).
[24] J. Adam, Jr., H. Goller, and H. Arenhovel, Phys. Rev. C **48**, 370 (1993).
[25] R. Machleidt, F. Sammarruca, and Y. Song, Phys. Rev. C **53**, R1483 (1996).
[26] R. Machleidt (private communication).
[27] S. A. Coon and J. L. Friar, Phys. Rev. C **34**, 1060 (1986).
[28] H. Kamada and W. Glöckle, Phys. Rev. Lett. **80**, 2547 (1998).
[29] V. G. J. Stoks, R. A. M. Klomp, M. C. M. Rentmeester, and J. J. de Swart, Phys. Rev. C **48**, 792 (1993).
[30] W. Glöckle, T.-S. H. Lee, and F. Coester, Phys. Rev. C **33**, 709 (1986).
[31] M. H. Kalos and P. A. Whitlock, *Monte Carlo Methods* (Wiley, New York, 1986).
[32] N. Metropolis *et al.*, J. Chem. Phys. **21**, 1987 (1953).
[33] A. Arriaga, V. R. Pandharipande, and R. B. Wiringa, Phys. Rev. C **52**, 2362 (1995).
[34] V. G. J. Stoks, R. A. M. Klomp, C. P. F. Terheggen, and J. J. de Swart, Phys. Rev. C **49**, 2950 (1994).
[35] J. L. Friar, G. L. Payne, V. G. J. Stoks, and J. J. de Swart, Phys. Lett. B **331**, 4 (1993).
[36] R. Schiavilla *et al.*, Phys. Rev. C **58**, 1263 (1998).
[37] J. L. Forest (private communication).
[38] S. C. Pieper (private communication).
[39] A. Akmal, V. R. Pandharipande, and D. G. Ravenhall, Phys. Rev. C **58**, 1804 (1998).
[40] J. L. Forest, V. R. Pandharipande, S. C. Pieper, R. B. Wiringa, R. Schiavilla, and A. Arriaga, Phys. Rev. C **54**, 646 (1996).
[41] E. Beise and C. W. de Jager (private communication).